

Practical characterization of eolian reservoirs for development: Nugget Sandstone, Utah–Wyoming thrust belt

SANDRA J. LINDQUIST

Amoco Production Co., P.O. Box 800, Denver, CO 80201 (U.S.A.)

(Received July 14, 1986; revised and accepted September 9, 1986)

Abstract

Lindquist, S.J., 1988. Practical characterization of eolian reservoirs for development: Nugget Sandstone, Utah–Wyoming thrust belt. In: G. Kocurek (Editor), Late Paleozoic and Mesozoic Eolian Deposits of the Western Interior of the United States. *Sediment. Geol.*, 56: 315–339.

The Jurassic eolian Nugget Sandstone of the Utah–Wyoming thrust belt is a texturally heterogeneous formation with anisotropic reservoir properties inherited primarily from the depositional environment. Original reservoir quality has been reduced somewhat by cementation and slightly enhanced by dissolution. Low-permeability, gouge-filled micro-faults compartmentalize the formation, whereas intermittently open fractures provide effective permeability paths locally.

Where productive, the Nugget Sandstone ranges from approximately 800 to 1050 ft (244–320 m) thick at subsurface depths of 7500 to 15,000 ft (2286–4572 m). Porosity ranges from several percent to 25%, and permeability covers five orders of magnitude from hundredths of milliDarcies to Darcies. Some Nugget reservoirs are fully charged with hydrocarbons.

Different stratification types have unique depositional textures, primary and diagenetic mineralogies, and deformational fabrics resulting in characteristic porosity, permeability, permeability directionality, and pore geometry attributes. Such characteristics can be determined from core analysis, mercury injection, nuclear magnetic resonance, conventional log, dipmeter and production data.

Nugget dune deposits (good reservoir facies) primarily consist of grainflow and wind-ripple cross-strata, the former of which have the better reservoir quality and the lesser heterogeneity in bedding texture. High-permeability facies are commonly affected by local quartz and nodular carbonate cementation, chlorite (and lesser illite) precipitation, and minor framework and cement dissolution. Gouge-filled micro-faults are the predominant deformational overprint.

Interdune, sand-sheet, and other water-associated deposits (poor reservoir facies) are characterized by low-angle wind-ripple laminae and more irregular bedding, some of which is associated with damp or wet conditions. Water-associated Nugget stratification generally contains the finest grained depositional textures and has the poorest reservoir properties. These non-dune facies contain intergranular micritic carbonate and illite precipitates and are most affected by compaction and pressure solution phenomena. Open types of fractures are somewhat more likely in this lower permeability rock.

Depositional models incorporating dune morphologies, facies distribution, permeability directionality, and theoretical concepts regarding dune migration through time are useful in delineating correlative intervals most likely to have continuity and potential communication of reservoir properties. Stratigraphic models can be adapted for reservoir simulation studies and also can be utilized in solving structural resolution problems if correlatable vertical sequences and relatively consistent cross-strata orientations exist.

Introduction

The geography, climate and tectonic setting of the western United States were favorable for the development of extensive eolian systems during much of the late Paleozoic and early Mesozoic eras (e.g., Peterson, 1980; Kocurek and Dott, 1983; Marzolf, this volume; Blakey, this volume).

The Jurassic eolian Nugget Sandstone of the Utah-Wyoming thrust belt is a prolific hydrocarbon reservoir, productive in nine structural fields along the leading edge of the Absaroka thrust plate (Fig. 1). The formation is a major

eolianite that, along with its probable equivalents such as the Navajo Sandstone, spans an area from northern Wyoming southward into Arizona and eastward into Colorado. From north to south these Nugget thrust belt producing fields are Ryckman Creek, Clear Creek, Painter Reservoir, East Painter Reservoir, Glasscock Hollow, Chicken Creek, Besie Bottom, Anschutz Ranch East and Pineview. Production occurs at depths ranging from approximately 7500 to 15,000 ft (2286–4572 m), and source for the hydrocarbons is thought to be contiguous, subthrust Cretaceous shales (Warner, 1980).

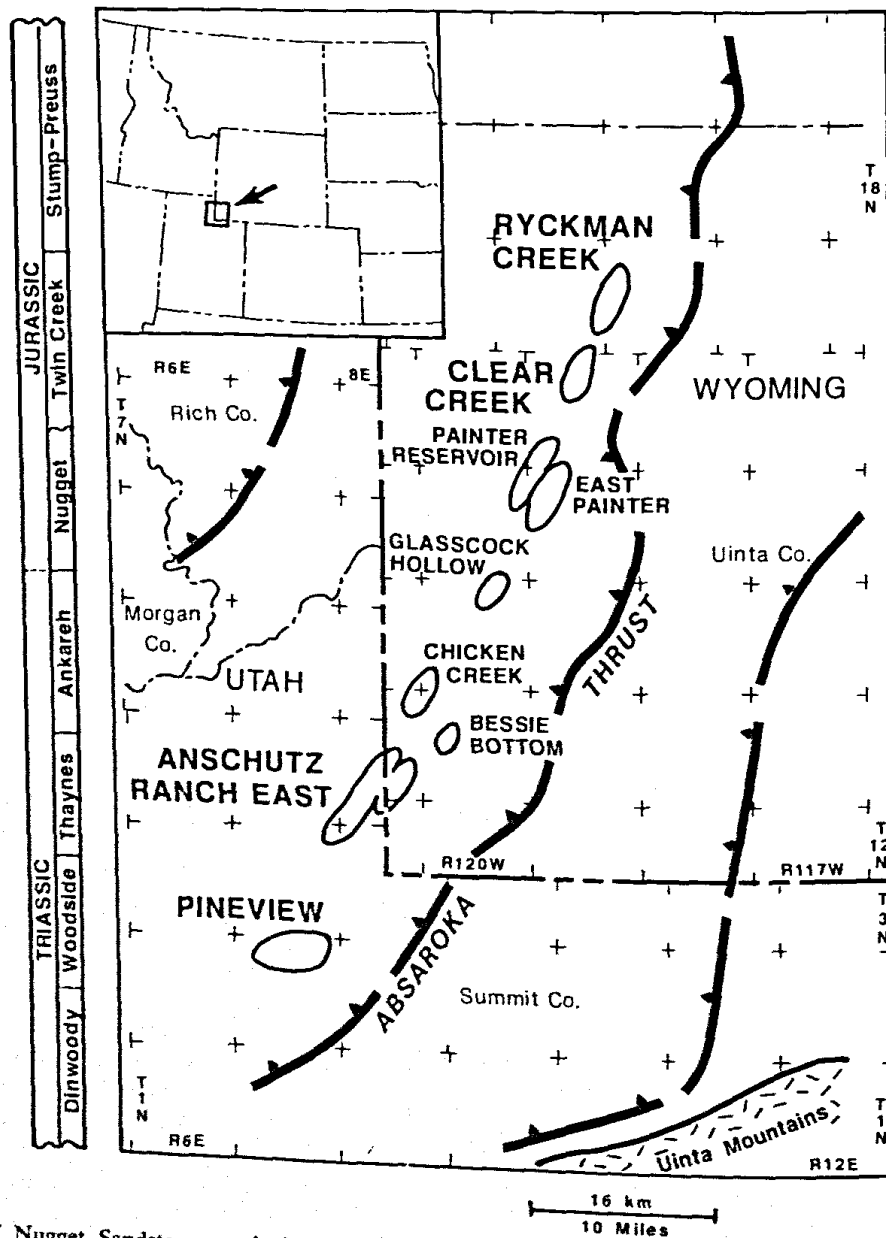


Fig. 1. Location of Nugget Sandstone producing fields in the Utah-Wyoming thrust belt. Stratigraphic position within the Triassic-Jurassic sequence is also shown.

The Nugget Sandstone overlies redbeds of the Triassic Ankareh Formation and is unconformably overlain by the Middle Jurassic Twin Creek Limestone (Fig. 1). The formation ranges in thickness from about 800 to 1050 ft (244–320 m) along the productive trend and consists entirely of highly quartzose sandstone with minor siltstone. Several tens of feet (± 10 m) erosional relief can be documented locally at the post-Nugget unconformity.

Formation porosity ranges from several percent to approximately 25%, and maximum horizontal permeability covers five orders of magnitude from hundredths of milliDarcies to slightly more than a Darcy. Reservoir properties are generally poorer toward the base of the formation, and a pronounced permeability directionality results from the predominantly cross-stratified sandstone texture.

Efficient exploitation of these reservoirs is complicated by the heterogeneity of the reservoir rock, locally complex structural configuration, and the nature of the contained hydrocarbons. Optimal development hinges on obtaining a detailed understanding of reservoir complexity and on consolidating that information into whatever level of detail is appropriate for the scale of problem being addressed.

Data presented in this paper are a synthesis of several subsurface Nugget field studies that were undertaken to improve our understanding of this formation both for development and for equity determination concerns. The studies incorporated subsurface well logs, cores, and production data. Emphasis in this paper is on the descriptive depositional characteristics of the rock because they apparently are of primary importance in controlling reservoir quality distribution and production performance in the study area. Of critical concern is the need to make heterogeneous reservoir descriptions practical enough to handle logically, yet accurate enough to predict and match production performance.

Study area and data base

Primary sources of data reported here are subsurface log suites and approximately 7200 ft (2200

TABLE 1

Nugget continuous core data utilized

Well	Continuous footage
Anschutz Ranch East Field	
W16-30	1074 ft (327 m)
W20-06	1052 ft (321 m)
W20-16	1812 ft (552 m) *
W29-04	177 ft (54 m)
	237 ft (72 m)
W29-12	1104 ft (337 m)
W36-16	319 ft (97 m)
	153 ft (47 m)
Clear Creek Field	
1-16A Mohawk	112 ft (34 m)
11-3B P.R.U.	287 ft (87 m)
23-9B P.R.U.	366 ft (112 m)
32-9B P.R.U.	31 ft (9 m)
East Painter Reservoir Field	
13-5A P.R.U.	394 ft (120 m)
Glasscock Hollow Field	
No. 1 Millis	59 ft (18 m)

* Includes penetration of vertical and overturned limb.

m) of core data from Clear Creek, East Painter Reservoir, Glasscock Hollow, and Anschutz Ranch East fields in Summit County, Utah and Uinta County, Wyoming (Fig. 1). Approximately 100 additional well logs with full Nugget penetrations also were examined for vertical sequence from other Nugget fields and from the surrounding area (T12-21N, R115-121W in Wyoming and T2-12N, R4-13E in Utah). Table 1 lists the continuous footage of core utilized from each field well. Most useful sequences were those exceeding 1000 ft (300 m) in thickness from Anschutz Ranch East Field.

Whole-core and/or plug porosity and air permeability data were obtained (at standard conditions) for all cores, as well as selected mercury injection (capillary pressure) and nuclear magnetic resonance analyses discussed in the text. Plugs utilized for reservoir quality measurement were 1 in. (2.5 cm) diameters and lengths, whereas whole-core samples were 3–4 in. (8–10 cm) diameters and 6–8 in. (15–20 cm) lengths. Dipmeter data were commonly acquired during logging runs and were of varying usefulness in this study.

Reservoir description

Dune, interdune, sand-sheet and other associated facies can be identified by stratification sequence in Nugget Sandstone cores.

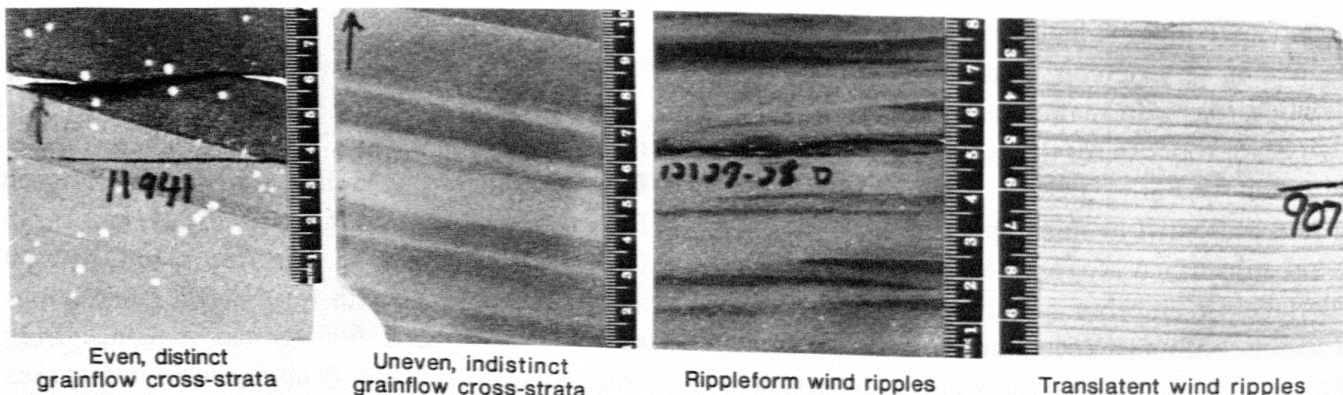
Dune deposits

The most important Nugget reservoir facies consist of dune deposits, with characteristic cross-stratification resulting from lee-face processes described by Hunter (1977, 1981). *Grainfall* deposits (grains falling to the lee face in the zone of flow expansion or separation) have poor preservation potential on large dunes because they are concentrated in an unstable area just lee to the dune crest and become incorporated in avalanching (although on smaller dunes or in strong wind regi-

mes, grainfall can occur over a much broader area). Grainfall deposits are not well-documented in the Nugget Sandstone within the study area. Avalanching or *grainflow* redistributes sand in a looser packing arrangement to a more stable location down the slipface where preservation potential is higher. Some lee faces with greater slope stability are completely reworked by deflected or reversing winds into tightly packed *wind-ripple* cross-stratification.

In subsurface core slabs, the most easily recognized and most commonly preserved Nugget dune cross-sets result from wind-ripple or grainflow processes, and these strata have several characteristic textures. Wind-ripple cross-strata (seen in Fig. 2 with lower-angle inclination) are composed of thin, inversely graded laminae that may preserve ripple-form shape or that may appear paral-

DRY STRATIFICATION TYPES



WATER-INFLUENCED STRATIFICATION TYPES

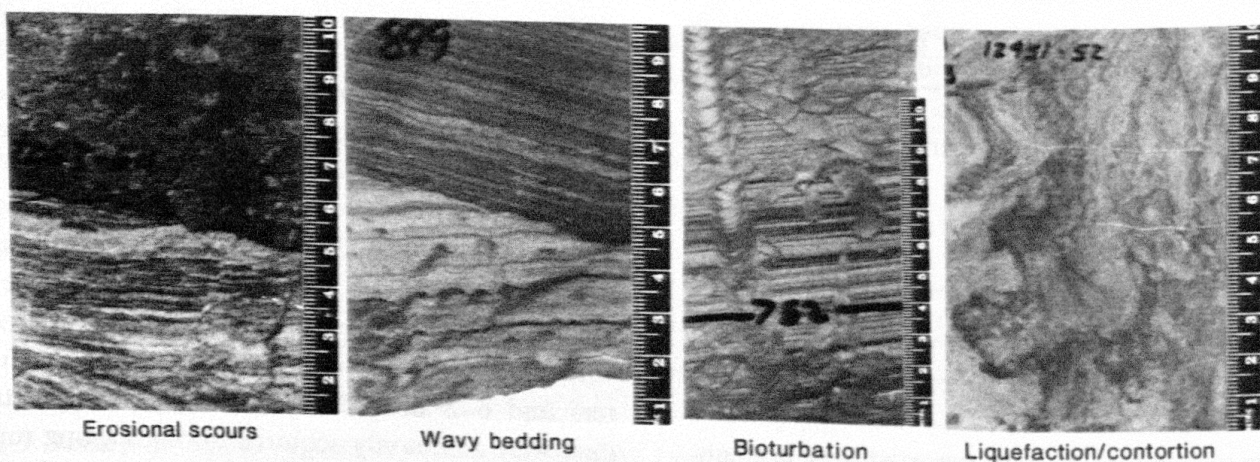


Fig. 2. Nugget major stratification examples.

lel-bedded (translatent strata; Hunter, 1977). Wind-ripple-generated strata will be discussed further with respect to interdune and sand-sheet deposits.

Nugget grainflow deposits are either visually distinct and even-textured, or more visually indistinct and uneven in appearance (Fig. 2). The even, distinct bedding is interpreted to result from grainflow of non-cohesive dry sand. This type of stratification has looser packing and higher porosity and permeability than the uneven, indistinct variety. Indistinct, uneven grainflow strata might result from post-depositional partial liquefaction, a process that could account for the uneven appearance of laminae and also perhaps for subtle differences in grain packing that reduce porosity and permeability. No obvious textural (grain size and sorting) differences were apparent in a comparison of several examples of the two types of grainflow strata from the same burial depths, but quantitative petrographic statistical comparisons were not attempted.

Dune cross-sets with the best reservoir properties, thickly laminated grainflow deposits, appear relatively homogeneous in the photomicrograph of an Anschutz Ranch East example, in which they have porosity in the 16–17% range and whole-core permeability equal to hundreds of millidarcies in all measured directions (Fig. 3A). Individual grainflow layers reach a maximum of 1–2 cm thicknesses within this sequence. Considering all Nugget grainflow strata in the thrust belt producing trend, porosity ranges from approximately 5 to 25% (average 12–13%), and arithmetic average horizontal permeability ranges from several millidarcies to hundreds of millidarcies. This regional variability in grainflow reservoir quality, especially permeability, can be partly explained by difference in parameters such as grain size and maximum depth of burial (Lindquist, 1983), in addition to the possible liquefaction packing differences previously discussed. Effective directional permeability ratios within amalgamated grainflow deposits approach 1.0 (at surface conditions) if there is minimal grain size and sorting variability within each grainflow layer and if no wind-ripple laminae separate the individual grainflow strata. Such textural homogeneity over considerable

vertical or lateral distance (e.g., between two wells) is unlikely, however, and significant directional anisotropy is more likely to exist.

Total microporosity, and thus the overall size of the pore system, can be estimated from nuclear magnetic resonance (NMR) data plotted as percent relaxation versus time (Fig. 3). In this procedure, hydrogen protons in water-saturated pores within a known magnetic field are reoriented to a second magnetic field. A signal amplitude and a time function are measured as the protons realign back to the original field. Amplitude is a function of total pore volume, and rate of amplitude decrease is a function of pore size. Longer relaxation times (a more horizontal curve) correspond to larger pore systems. The circled numbers in Fig. 3 are dimensionless relative indices of the total amount of microporosity in the pore system and are for comparison purposes only. The index reflects the proportion of pores with $< 0.17 \mu\text{m}$ diameter (corresponding to the proportionate amount of relaxation occurring within 0.05 s).

NMR data from Fig. 3A illustrate that dune grainflow strata are predominated by macro-pore systems. Efficient grainflow pore systems with large pore *throats* also are characterized from mercury injection data, presented as displacement pressure versus percent mercury (non-wetting fluid) saturation. Connate pore fluids are easily displaced to an irreducible saturation of approximately 10%, with only low entry pressure required. Thus, as much as 90% of the connate water in this type of rock can be displaced by minimal pressure (or a relatively small column of non-wetting fluid such as hydrocarbon).

Dry interdune and sand-sheet deposits

Nugget interdune and sand-sheet deposits are characterized by an abundance of low-angle, wind-ripple-generated strata (Fig. 2), typical of similar facies described by Fryberger et al. (1979, 1983); Ahlbrandt and Fryberger (1981); Kocurek (1981); and Kocurek and Nielson (1986). If not associated with water in the depositional environment or adversely affected by diagenesis, reservoir properties can still be relatively good in low-angle wind-ripple strata from interdunes and sand sheets

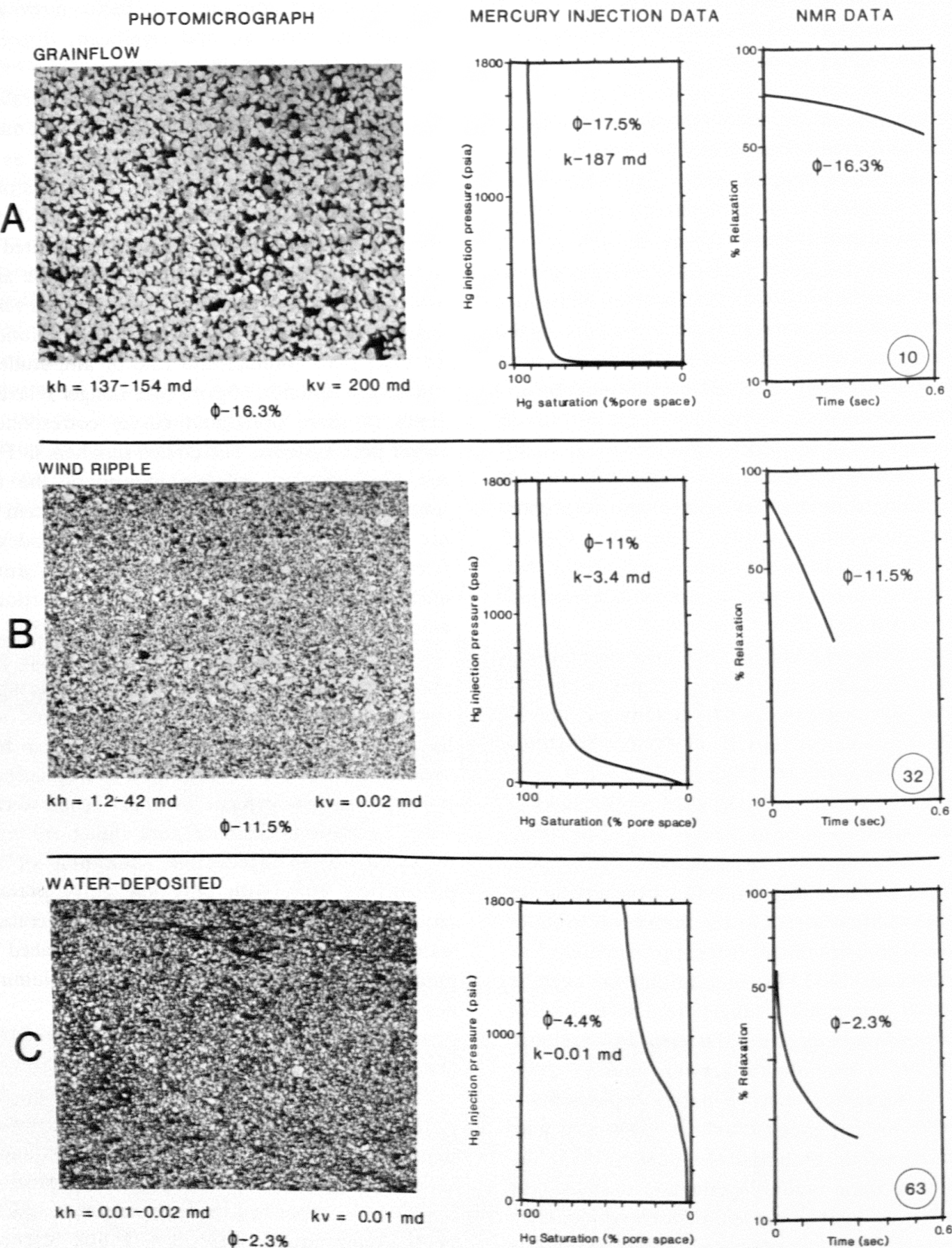


Fig. 3. Characterization of some major facies-related stratification types from Anschutz Ranch East Field. Porosity (ϕ , percent), whole-core permeability (kh = horizontal, kv = vertical, milliDarcies), nuclear magnetic resonance (NMR) data, and mercury injection data are illustrated. The circled number is a microporosity index derived from NMR data. NMR and mercury injection analyses were not performed on the exact same sample photographed. (A) Grainflow; (B) wind ripple, (C) water-deposited.

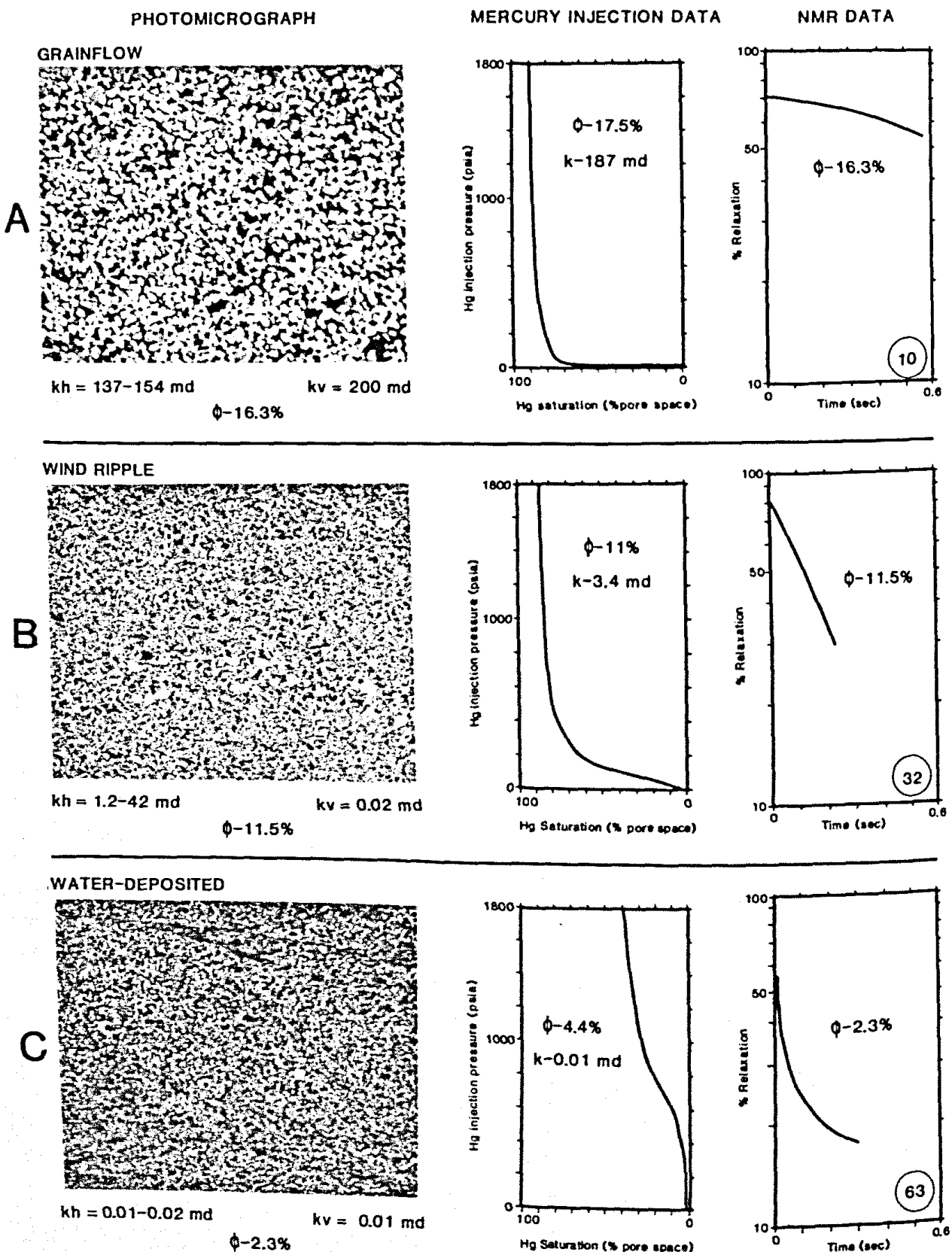


Fig. 3. Characterization of some major facies-related stratification types from Anschutz Ranch East Field. Porosity (ϕ , percent), whole-core permeability (k_h = horizontal, k_v = vertical, millidarcies), nuclear magnetic resonance (NMR) data, and mercury injection data are illustrated. The circled number is a microporosity index derived from NMR data. NMR and mercury injection analyses were not performed on the exact same sample photographed. (A) Grainflow; (B) wind ripple, (C) water-deposited.

(similar to reservoir quality in wind-ripple deposits comprising lee face cross-strata).

Wind-ripple deposits in Fig. 3B appear texturally heterogeneous in the photomicrograph with porosity < 12% and directional whole-core permeability ranging from several milliDarcies to tens of milliDarcies horizontally. Vertical permeability is just hundredths of milliDarcies, and this pronounced directional disparity is inherent to ripple-generated bedforms because of their inversely graded structure. The degree of directional permeability disparity is highly variable in wind-ripple deposits because of the range of textural characteristics they can possess.

Overall size of the pore system within the wind-ripple deposit is somewhat smaller than that for the grainflow example, as indicated by the higher NMR microporosity index of 32. Mercury injection data document somewhat less efficient displacement of connate pore fluids through smaller pore throats (requiring greater entry pressure, or a larger hydrocarbon column), but ultimate irreducible saturation is still < 15%. In the thrust belt producing trend, porosity in Nugget wind-ripple strata ranges from about 3 to 12% (average 7–8%), and arithmetic average horizontal permeability is commonly ≤ 1 mD (with a range from hundredths to tens of milliDarcies).

Dune-interdune cycles

Reservoir quality variability associated with a typical dune-interdune vertical configuration is illustrated for the distinct, even grainflow deposits (Fig. 4a) and the indistinct, uneven variety (Fig. 4b), both from essentially the same burial depths. Wind ripples at the base of each cycle grade upward into thicker grainflow cross-strata that are truncated by the next overlying interdune deposit at a first-order bounding surface. In this example, distinct grainflow cross-strata have porosity of 15–18% and whole-core permeability primarily > 10 mD. Indistinct grainflow cross-strata have 12–15% porosity and generally < 10 mD maximum permeability. Basal wind-ripple strata in both sequences have porosity < 10% and permeability of tenths to hundredths of milliDarcies, with notable directional disparity.

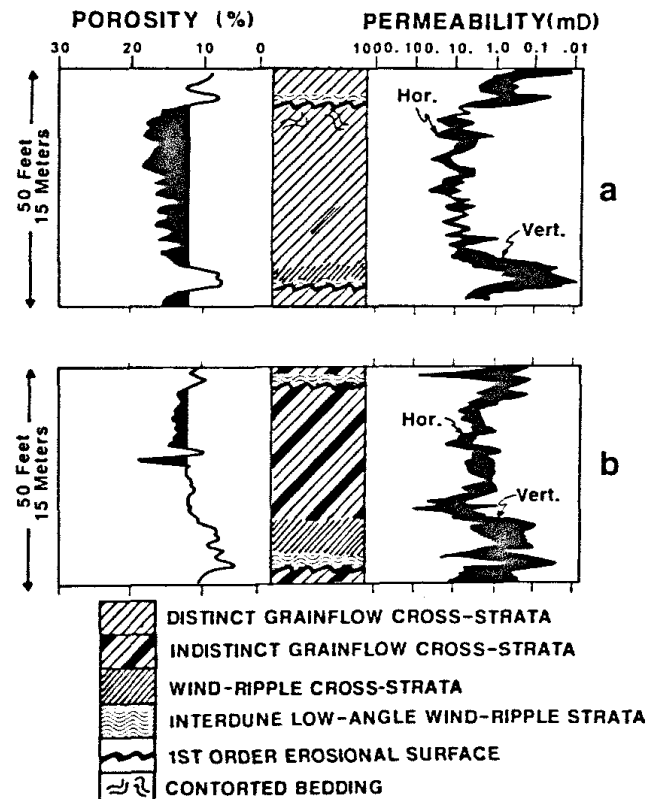


Fig. 4. Reservoir quality comparison of dune-interdune sequences for the distinct, even type of cross-strata (a) and the indistinct, uneven variety (b). Reservoir properties are best in the former texture. Porosity $> 12\%$ is shaded, as is the disparity between vertical and horizontal permeability.

Water-associated deposits

Other modified or associated deposits in the eolian environment result from the presence of water (e.g., high ground-water tables or surficial water movement) (Fig. 2). Ahlbrandt and Fryberger (1981) summarized typical characteristics of these facies. High water tables can entrap fine-grained material and result in precipitation of early diagenetic minerals, especially carbonates or evaporites. Soft-sediment deformation and bioturbation by plants and animals in some cases homogenizes the stratification, and significantly different textures of sediment can be introduced to the environment.

No visible porosity remains in the wet interdune deposits in Fig. 3C. Measured porosity is $< 5\%$, and all directional whole-core permeability is ≤ 0.02 mD. Effective directional permeability ratios commonly approach 1.0 (at surface conditions) in such facies. The NMR microporosity

index is 63, and connate waters cannot be efficiently displaced, even with high pressure (a large hydrocarbon column). Ultimately, 60–70% irreducible and immovable connate water will remain bound in this rock because the pores and pore throats are so small.

Regionally, Nugget Sandstone “wetter” fabrics have porosity ranging from approximately 2 to 9% (average 5–6%) with arithmetic average maximum permeability of several hundredths of a millidarcy (ranging to approximately 1 mD). Whether or not this facies creates a barrier to either initial hydrocarbon migration or to production-related fluid movement depends to a large extent on continuity of the barrier facies, reservoir fluid characteristics, fluid pressure differentials, and time. More viscous fluids and lesser time (e.g., geologically instantaneous production rates) maximize the effectiveness of this facies as a barrier or hindrance to flow.

Nugget vertical sequence

Vertical sequence in the formation is illustrated in Fig. 5 with a gamma-ray and wireline-log porosity plot for the W29-12 well in Anschutz Ranch East Field. Reservoir quality gradually improves from the base of the formation upward through the lower two-thirds where, in many field wells, there is an abrupt porosity break. This overlying lower porosity interval is absent in the northern part of the productive trend partly because of facies changes and partly because of erosional removal at the post-Nugget unconformity.

The lower third of the formation consists of sandstone that was deposited largely in a low-relief, sand-sheet environment characterized by small isolated dunes and locally poor drainage. Wind-ripple strata are the predominant sedimentary structure, associated with less common wavy (or crinkly) bedding, bioturbation, scouring, and soft-sediment deformation. Some of the coarsest material in the eolian depositional environment is present in this interval as isolated rippleforms, but for the most part, overall grain size is quite fine. The section is commonly dark red because of the presence of hematitic clay coatings on the sand grains.

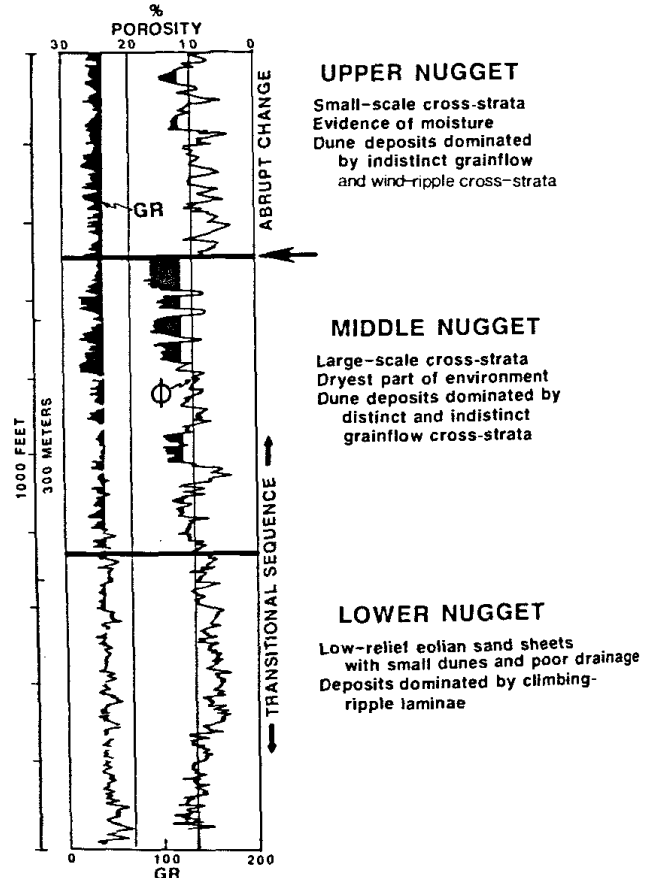


Fig. 5. Nugget vertical sequence from the W29-12 well in Anschutz Ranch East Field, as characterized by porosity and gamma-ray parameters.

As summarized by Kocurek and Nielson (1986), sand-sheet development is favored over major dune formation if factors such as high water tables, surface cements, vegetation, flooding, and/or coarse grain size characterize the depositional environment.

Speculation about the origin of the basal Nugget sand sheets remains inconclusive from the focus of this study. There is certainly evidence for locally high water tables from the abundance of faunal bioturbation observed and from the amounts of fine-grained (infiltrated?) interstitial hematitic material and (early?) micritic carbonate detected. Some of the irregular or wavy stratification could have been originally associated with early evaporites, but direct evidence for evaporite presence was not documented. Roots or root casts were not observed, but essentially massive or somewhat mottled intervals in this basal part of the formation could be the result of the presence of vegetation. Armored lag surfaces (isolated,

coarse-grained rippleform strata) locally may have helped to prevent the formation of larger scale dunes, but coarse-grained sediment and obvious wadi deposits are not prevalent throughout the interval.

The lower third of the Nugget Sandstone is transitional to the middle third where best reservoir properties are developed in dune grainflow deposits within stacked dune-interdune sequences. Largest preserved dune sets from the driest part of the depositional environment characterize this middle interval, but extreme lateral variability also occurs within this zone. Middle Nugget sand-sheet deposits generally are not red and rarely are associated with water-influenced fabrics.

The porosity break between the middle and upper third of the formation corresponds to a (climatically caused?) change to thinner sets of cross-strata primarily composed of indistinct grainflow and wind-ripple deposits, and more evidence for the presence of moisture in the depositional environment. In some wells the porosity break is associated with underlying soft-sediment deformation and may represent a local pseudo-time line.

Porosity-permeability relationships

Based on a number of descriptive *and associative* core criteria, at least seven Nugget stratification categories with varying porosity and permeability can be catalogued in Anschutz Ranch East Field (Fig. 6), but for petrophysical purposes they can be combined into two main populations. Two major "rock type" populations were first proposed by Stan Kolodzie in Amoco's Production Department from porosity and water saturation crossplots of log-derived data. The first population is a series of low-angle stratification types (largely red) associated with wet interdunes and low-relief sand sheets. The second population consists of dune cross-strata and lower-angle wind-ripple deposits not affected by water presence.

Population one (non-dune origin) includes low-angle, red wind-ripple strata [rippleform (No. 1) and thin (< 5 mm) translatent (No. 2)], as well as thicker (> 5 mm) translatent strata (No. 3) and

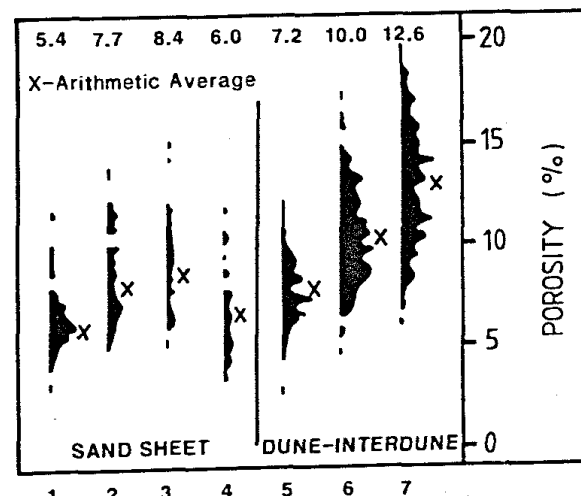
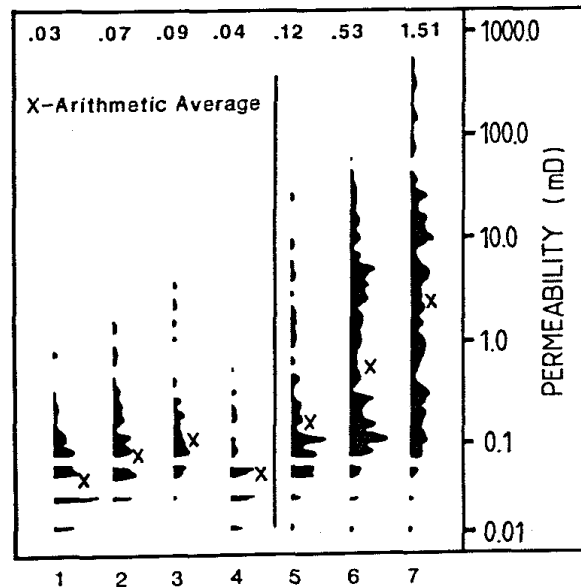


Fig. 6. Porosity and permeability distribution for seven Nugget stratification categories distinguished by descriptive and associative core criteria at Anschutz Ranch East Field. Types 1–4 are red and are most common in lower Nugget sand-sheet or wetter interdune facies. Types 5–7 are not red and are typical of middle to upper Nugget dune-interdune cycles. Approximately 1500 plug samples are represented in the data. See text for further discussion.

extensively bioturbated or wavy laminae (No. 4). Population two (dune and dry interdune origin) includes grainflow and wind-ripple cross-strata of varying thicknesses (No. 7 > 5 mm, No. 6 < 5 mm), as well as associated low-angle wind-ripple laminae (No. 5) that are not red. A red hematite stain was probably ubiquitous to most of the formation early in its burial history, as per ideas of Walker (1979), but it is now most intense in, or in some places restricted to, finest-grained inter-

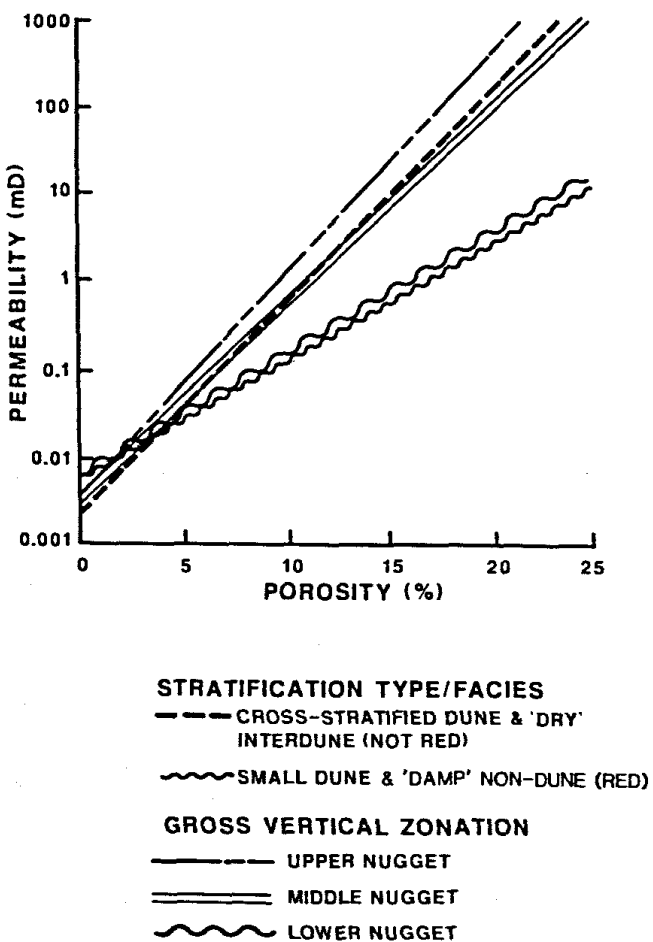


Fig. 7. Semi-log cross plot of permeability and porosity for Anschutz Ranch East Field vertical zonation and for major petrophysical populations of strata. Two main relationships are apparent.

vals of low permeability, many of which show evidence for the presence of water in the depositional environment. Presumably, oxidized iron may have been removed from the more permeable intervals by subsurface fluid movement.

The two petrophysical populations are distinguishable in permeability–porosity cross plots for Anschutz Ranch East Field (Fig. 7) where those populations correspond to the gross vertical zonation of the formation previously discussed. Sandstone in the lower third of the formation has a porosity–permeability relationship similar to that of the sand-sheet or non-dune stratification types, whereas porosity–permeability relationships from the upper two-thirds of the formation correspond better to that of the dune and dry interdune population. Note that for equal porosity values, permeability for the two petrophysical populations is generally quite different.

Diagenetic modifications

Nugget reservoirs have undergone diagenesis that can be related to depositional criteria, burial history, tectonism, and oil migration (Lindquist, 1983). Major diagenetic events include compaction and local pressure solution; cementation by quartz, ferroan and non-ferroan carbonates, illite and chlorite; dissolution of carbonates and silicates; and alteration of hydrocarbons. Hydrocarbon inclusions are found in some cements.

The most porous and permeable facies (dune and dry interdune deposits) contain quartz overgrowths and zoned, nodular sparry carbonate cements, as well as authigenic chlorite and illite. Cements are generally only locally abundant. Dissolution of small volumes of carbonate cement and silicate framework grains also occurred.

Lower-permeability facies (from sand-sheet and wetter environments) contain a greater abundance of detrital clays, authigenic illite and probable early micritic carbonate cements. Chlorite is rare or absent. Early cements in wet eolian environments have been recently documented by Krystnik et al. (1985). Pressure solution and compaction phenomena are also locally more common in low-permeability facies.

Late diagenetic events, probably related in time to the migration of hydrocarbons or their precursors, involve the precipitation of iron-rich diagenetic products (including chlorite and ferroan dolomite) in open fractures and in intergranular pores. Some ferroan dolomite contains fluorescent hydrocarbon inclusions. Iron was probably mobilized from hematite in permeable zones because those intervals are generally the most "bleached" in color now. Diagenetic fronts involving these ferroan minerals are commonly observed and are related to depositional permeability differences in the sandstone framework or to deformationally caused permeability changes. Black hydrocarbon residues or asphaltenes were emplaced or precipitated locally after most diagenetic cementation had occurred, but possibly prior to a late stage of carbonate dissolution.

The net result after diagenesis is still a rock with reservoir properties largely determined by facies and texture (i.e., reservoir quality distribu-

tion closely mimics facies configuration). Dune cross-strata from the driest parts of the depositional environment probably always have had and still have best reservoir quality, whereas facies associated in some fashion with water always have had and still have the worst properties. Such a direct relationship may not always exist, especially in Paleozoic wetter dune deposits extensively cemented early in their burial histories. For example, Helmold and Loucks (1985), and others, report that eolian sandstone porosity in the Minnelusa Formation is largely secondary, resulting from dissolution of early gypsum or anhydrite cements during structurally controlled, regional flushing events.

Tectonic overprints

Tectonic activity not only reorients the rock, but also results in fracture and micro-fault formation that can affect the distribution and/or movement of hydrocarbons in the system. Gouge-filled micro-faults, produced by shearing and pulverization of porous rock framework, create potential major barriers to fluid movement. This pulverized framework material is dominated by microporosity, and micro-faults as thin as a fraction of a millimeter can reduce permeability to air (at surface conditions) by an order of magnitude or more in the best reservoir rock (Lindquist, 1983, East Painter Reservoir Field). Intervals with poorer reservoir properties in some cases are more characterized by open fractures that either become completely mineralized (typically by ferroan carbonates in Nugget fractures), or that remain at least partially open and able to transmit fluids through an otherwise low-permeability system.

Fracture and fault formation cause at least some compartmentalization of the reservoir and restriction of fluid movement, which can impact reservoir performance. Predicting the density and distribution of fractures and faults is risky in the subsurface because exact structural configurations are difficult to determine, and multiple episodes of fracture/fault formation associated with different stress regimes might have occurred (e.g., Laramide compression versus later Tertiary extension; fig. 7 in Lindquist, 1983). In some cases, production

anomalies unexplained by depositional or diagenetic reasons can be used to postulate the presence and locations of fractures or faults in structural trap fields.

Most Nugget fracturing and faulting is probably associated with formation of the producing field structures and therefore predates hydrocarbon migration. However, fluorescent hydrocarbon inclusions are found in gouge-filled micro-faults and in dolomite fracture fills, their presence indicating partial time overlap between faulting/fracturing and hydrocarbon migration.

Facies recognition from subsurface logs

Eolian facies and rock types can be inferred from wireline log suites and vertical sequence, especially if they can be initially calibrated with core data. Reservoir properties and several log parameters are related to a typical Nugget dune-interdune depositional sequence in Fig. 8. In the left trace are gamma-ray and porosity curves plotted in a standard wireline format with dipmeter-derived stratigraphic bedding dip (GEODIP) plotted between them. Cross-strata dip decreases from about 20° SW at the top of the dune facies to horizontal at the bottom.

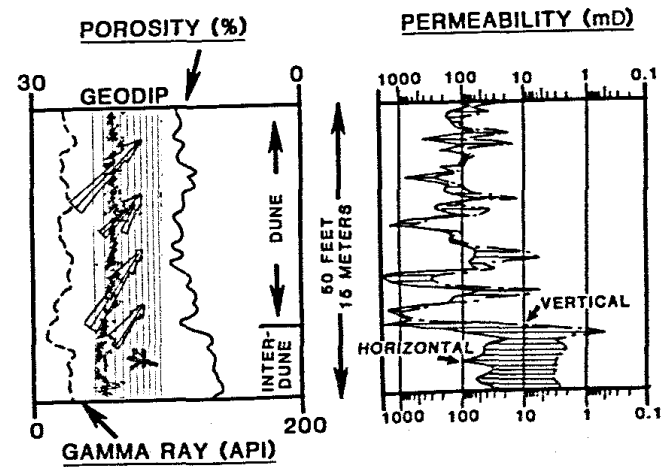


Fig. 8. Relationship of porosity, directional permeability, gamma ray and stratigraphic bedding dip (GEODIP) to dune-interdune sequence at Clear Creek Field. The difference between horizontal and vertical permeability is shaded to highlight directional disparity. In this example, the gamma-ray curve is less consistently diagnostic of facies than other parameters illustrated. Note that some of the best permeability is at the base of the cross-sets where coarsest-grained, basal grain-flow wedges are located (from Lindquist, 1983).

On the right side of Fig. 8, both horizontal and vertical plug permeability curves are plotted on a logarithmic scale covering four orders of magnitude from tenths of a milliDarcy to a Darcy. The difference between the horizontal and vertical values is highlighted to show directional anisotropy.

The dune deposit approximately 40 ft (12 m) thick is characterized by an overall decrease in porosity toward its base, as well as an increase in permeability anisotropy resulting from interbedding of the coarsest-grained, basal portions of permeable grainflow wedges with less-permeable, wind-ripple laminae of the dune margin or interdune. Both reservoir quality trends correspond to the decrease in bedding dip magnitude toward the bottom of the dune. The underlying interdune deposit is more horizontally bedded, has poorer

reservoir quality, and greater disparity between vertical and horizontal permeability.

For the Nugget Sandstone, porosity logs are good wireline tools to use for facies determination, but they are best used in conjunction with other logs such as the stratigraphic dipmeter and the gamma ray. Figure 9 illustrates one core segment where porosity data alone did not resolve dune-interdune sequences very well because the indistinct, uneven dune cross-strata have reservoir properties comparable to their associated interdune deposits.

The gamma-ray curve responds to primary and diagenetic mineralogic variability (especially potassium content in the Nugget Sandstone), which is at least partly related to grain size and therefore specific facies in the depositional en-

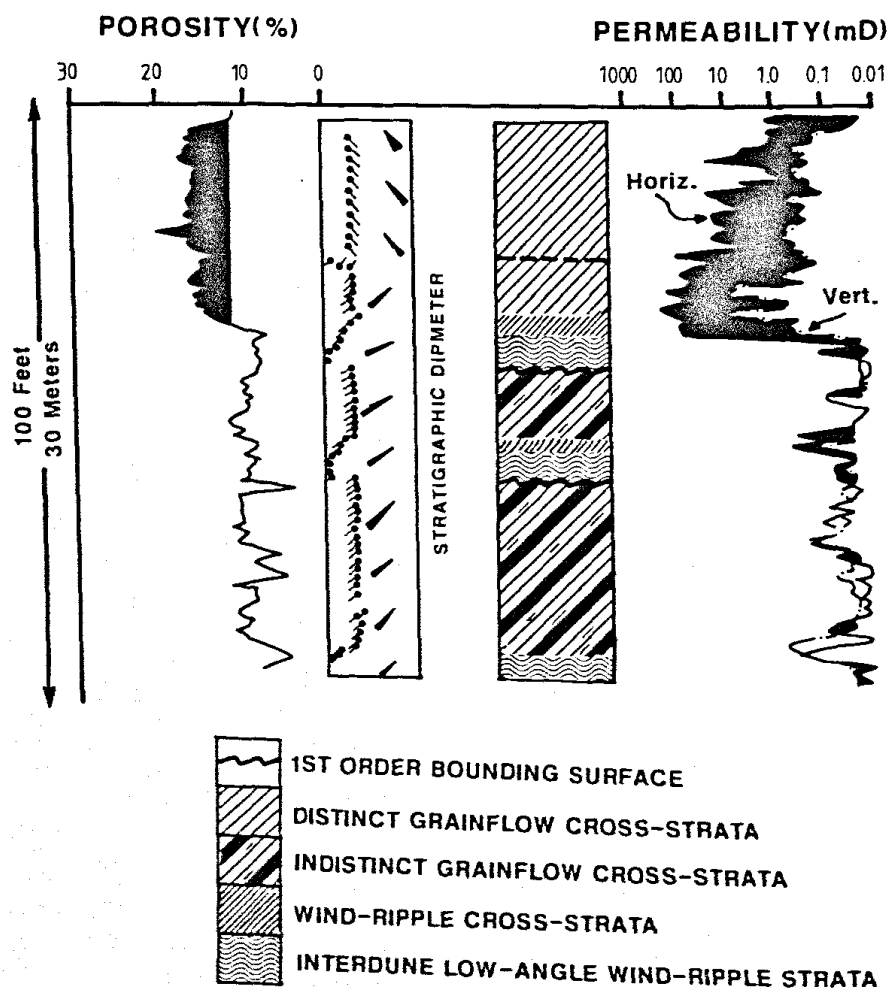


Fig. 9. Dune-interdune facies resolution. The two lower dune cross-set cycles distinguishable from stratigraphic dipmeter data are not easily resolved by porosity and permeability data because they are of the indistinct grainflow texture with reservoir properties similar to their associated interdune deposits. Also note the unusual directional dip variability (SE azimuth) in the porous Nugget cross-strata of the top cycle.

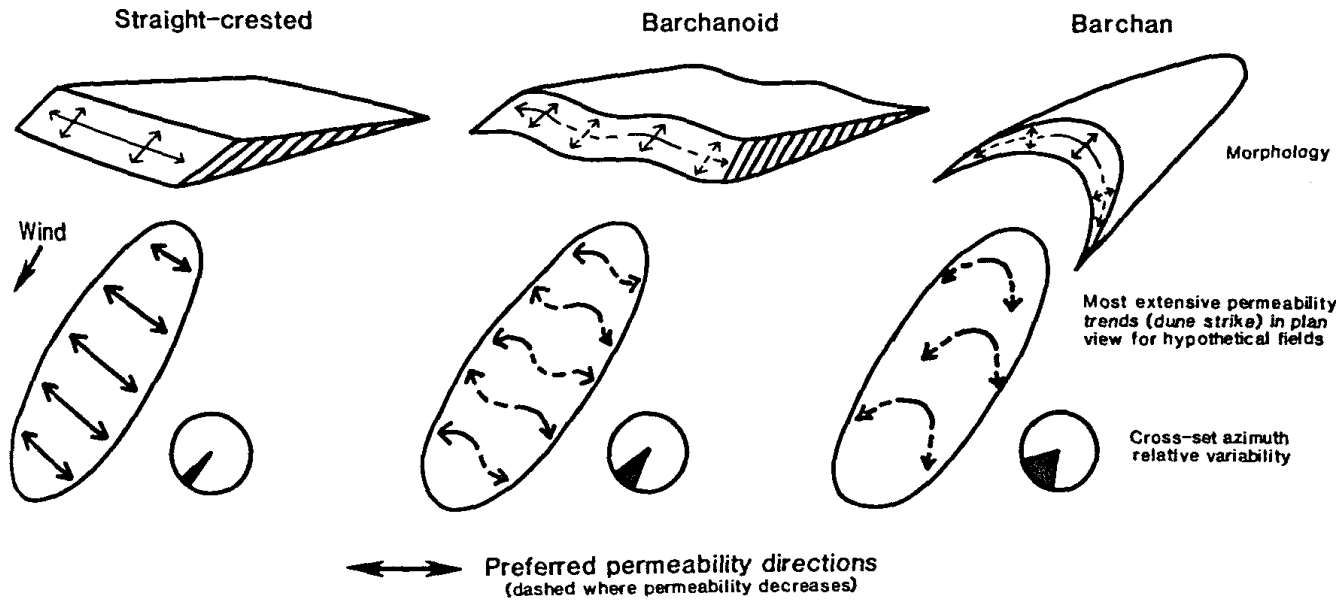


Fig. 10. Trend and continuity of preferred permeability directions for three common dune morphologies. Relative differences in azimuth variability for lee face cross-sets are also shown. Note the perpendicular relationship between bedding-plane dip azimuth and the trend of the most extensive permeability line.

vironment. Nugget sand-sheet and interdune facies are generally somewhat finer grained and more mineralogically immature (more feldspar and clay minerals) than the cross-stratified dune deposits, but not consistently enough to permit facies identification from the gamma ray curve alone. The low-porosity interdune facies distinguishable from porosity and dipmeter curves in Fig. 8 is not the only interval in the figure registering relatively high gamma-ray readings (indicating greater potassium content).

High-quality dipmeter data are valuable in describing eolian sequences where no structural reorientation has occurred. The term "stratigraphic dipmeter data" is used in this paper to differentiate depositional bedding strike and dip information from structural strike and dip data. Not only can depositional bedding dip *magnitude* be used to distinguish dune-interdune facies, but cross-strata dip *azimuth* also is useful in approximating dune morphology and delineating dune trend (Fig. 10).

For a predominantly unidirectional wind system, straight-crested transverse or oblique dune lee faces should have less azimuth variability than more sinuous-crested varieties. If a consistent and highly unidirectional depositional cross-strata dip azimuth is known to exist, that value can be

mathematically removed from standard dipmeter data in structurally reoriented, cross-stratified horizons to define or confirm structural dip and to document changes in structural dip within the cross-stratified interval. The procedure can be done easily on a stereonet or with a calculator, or a modified dipmeter log can be computer-generated. For much of the Nugget Sandstone in the thrust belt, a southwesterly depositional cross-strata dip is common, corresponding to the probable predominance of straight-crested or slightly sinuous-crested dunes in the rock record.

Quantification of permeability directionality

Because cross-strata recorded on the dipmeter are the preserved dune lee faces, it is possible to define their three-dimensional orientation, as well as the orientations of the bedding-parallel, preferred permeability directions associated with them (Fig. 10). Preferred permeability components have both value and distance (length) attributes. If any bedding-parallel direction is considered to have a constant permeability value, then the distance attribute becomes very important (assuming cross-sets are bounded by deposits of poorer reservoir properties).

The shortest, bedding-parallel permeability

component is oriented up and down the lee face (equal to that lee face dip length and restricted by the thickness of the preserved cross-sets). The longest bedding-parallel permeability component is oriented along the more extensive trend or strike of the dune (restricted by its morphology and lateral extent). This latter trend is perpendicular to the bedding-plane dip azimuth recorded on the stratigraphic dipmeter and is the most important permeability trend because of its potential extent.

Preferred permeability directions must be thought of as two-dimensional *lines* with trend and plunge, in contrast to three-dimensional bedding *planes* with strike and dip recorded as dipmeter data. The trends and continuity of the extensive strike-oriented permeability lines for three morphologies most commonly reported in ancient eolian systems are shown in plan view in Fig. 10. The plunge component is zero for these structurally undisturbed representations.

Preferred permeability directions can be quantified to some extent (Fig. 11). Height of the preserved dune deposit can be measured directly

from wireline log data as the true stratigraphic thickness of the porosity development associated with dune cross-sets. Several tens of ft (< 20 m) are common preserved thicknesses for Nugget dunes. Dip length of the lee face permeability line is calculated to be approximately three times the preserved height for the $\pm 20^\circ$ preserved cross-strata dip magnitudes typically encountered in the subsurface. In the Nugget Sandstone, this lee face dip dimension ranges from tens of feet or less to a maximum of perhaps 200 ft (< 10 to approximately 60 m) for thickest dune sets (usually compound cross-sets).

The more extensive strike dimension of the dune is difficult to predict unless well control is dense and lateral correlations can be believed with a high degree of confidence. Hundreds to perhaps thousands of feet (tens to hundreds of meters) might be reasonable lateral dimensions for many Nugget dunes.

The minimum permeability dimension across bedding can be extensive because it is obliquely parallel with the downwind path of dune migration (slipface advance) through time. Individual

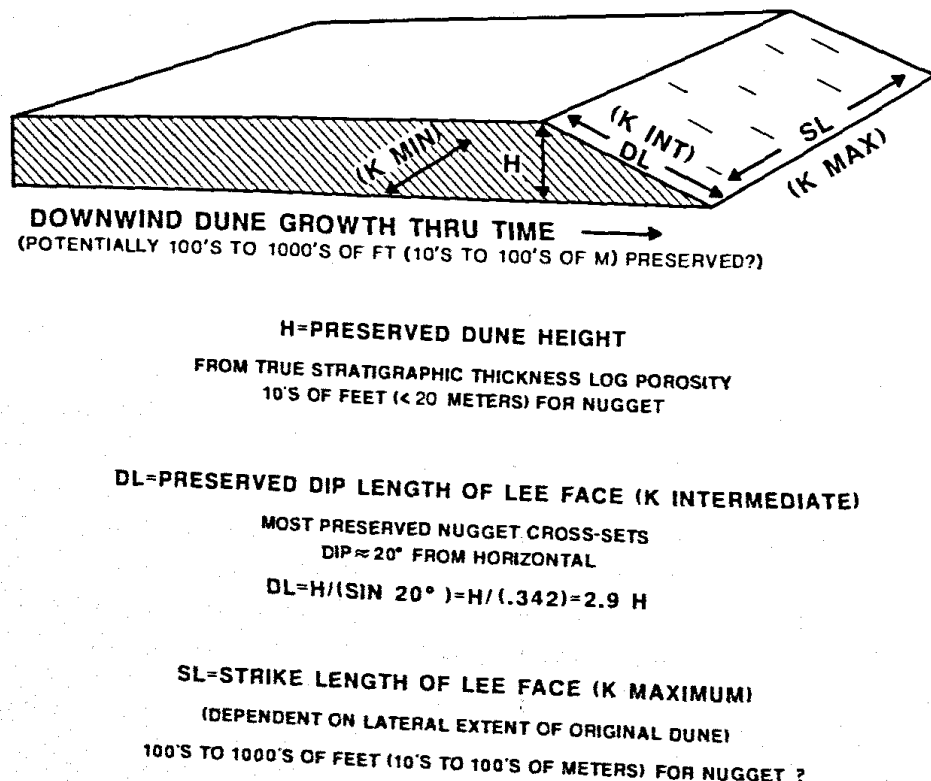


Fig. 11. Quantified preferred permeability dimensions for a hypothetical straight-crested dune.

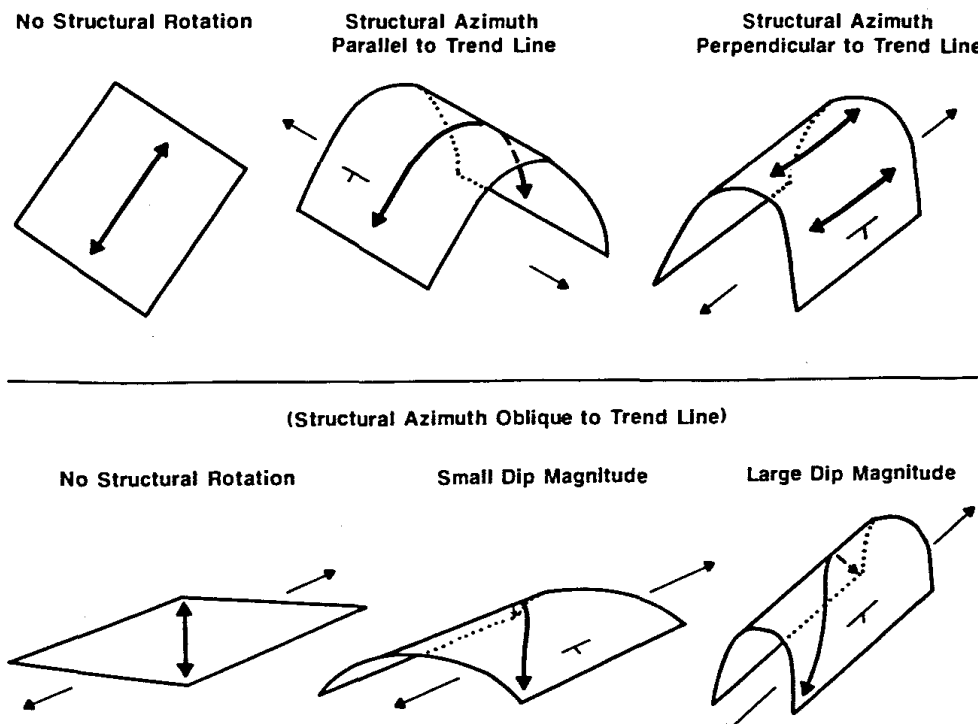


Fig. 12. The effect of structural rotation on trend and plunge of most extensive preferred permeability line. Relationship to strike and dip of the associated bedding plane is discussed in the text.

grainflow layers comprising the slipface cross-sets are likely to be separated by thin, low-permeability wind-rippled surfaces.

For the Nugget Sandstone, the most extensive preferred permeability direction is oriented NW-SE for structurally undisturbed sections. When structurally rotated parallel with its trend, this permeability line assumes a plunge equal to the structural dip magnitude and a (down-plunge) trend equal to the structural dip azimuth (Fig. 12). If rotated perpendicular to its orientation, trend and plunge of the line do not change; the effect is the same as rolling a pencil up and down an inclined surface. In these two cases, the *trend* of the permeability *line* is either exactly parallel with or exactly perpendicular to the bedding-plane dip azimuth recorded as dipmeter data.

With structural rotation oblique to the line, small structural dip magnitudes do not change the permeability trend appreciably, but a plunge component somewhat less than the structural dip magnitude (actually an apparent dip) is added. Greater structural dip magnitudes add a larger plunge component to the line and also deviate its trend more from the original configuration, eventually

approaching effective parallelism with the axis or strike of the structure. In this obliquely rotated situation, trend of the permeability line can no longer be determined directly from dipmeter bedding-plane data because that trend is now oblique to the dip azimuths recorded. Additional calculations must be made.

If the extensive preferred permeability direction becomes vertical or nearly vertical, drainage around a wellbore in a lateral sense becomes controlled by the shorter permeability trend associated with the lee face dip length and by the minimum permeability component across bedding (Fig. 13). If this cross-stratified interval is bounded by deposits of poorer reservoir quality, a narrow elliptical cylinder of effective drainage can be established around the wellbore, as is the case for the W32-04 well in Anschutz Ranch East Field.

Genetic layering and reservoir modeling

The migration through time of a dune or genetic interval that is bounded by associated deposits of poorer reservoir quality defines a correlatable unit which is likely to have best potential continuity

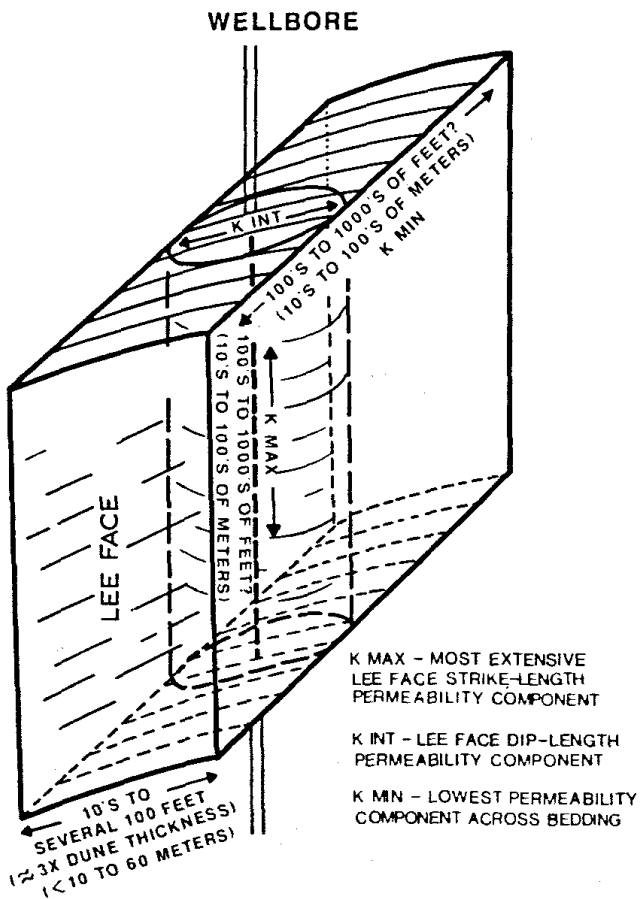


Fig. 13. Vertical structural orientation of a straight-crested dune. Lateral drainage around the hypothetical wellbore is controlled most by the permeability component associated with the lee face dip length.

and communication of reservoir properties. Two major hypotheses for net dune preservation, downwind climb (Rubin and Hunter, 1982) and water-table deflation (Stokes, 1968; Loope, 1985), are illustrated in Fig. 14.

The latter case requires subsidence, transgression or a "regional event" to create essentially horizontal bounding surfaces or deposits. Such bounding deposits are likely to consist of areally extensive evaporite or carbonate lithologies (such as in many Paleozoic eolianites in the western U.S.). Although these lithologic contrasts do not exist in the Nugget Sandstone, regional changes in the depositional environment through time affected sedimentation and reservoir quality, making it possible to correlate essentially flat "layers" on a large scale at Anschutz Ranch East Field. The *internal* composition of each "layer" in this water-table deflation model can be more complex

than illustrated (e.g., composed of downwind-climbing dune systems described below).

The upper examples in Fig. 14 illustrate the downwind climb of dune systems through time. In most cases, significant erosion of the original dunes probably has occurred. Bounding surfaces or interdune deposits separating these genetic units are not flat for correlation purposes. The "layers" in this model are slanted. Angle of downwind climb has been documented in the literature to be commonly $< 1^\circ$ for the Entrada Sandstone (Kocurek, 1981).

The downwind-climb ("slanted-layer") hypothesis was used to correlate two wells from opposite ends of Clear Creek Field (Fig. 15). Plotted for each well are gamma ray, stratigraphic dipmeter, porosity and permeability curves. The cross-section is hung from a postulated datum in the overlying Twin Creek Formation to correct for topographic relief at the post-Nugget unconformity. The potential correlation of major interdune bounding surfaces identified in cores and from log suites climbs in a southwesterly, downwind direction at an angle of 0.3° . Over the 1.9 mi (3.1 km) lateral distance, that small angle of climb makes a considerable vertical difference in the stratigraphic position of correlative horizons. Note the variability in reservoir properties and stratigraphic sequence within correlative intervals.

An approximation of the water-table ("flat-

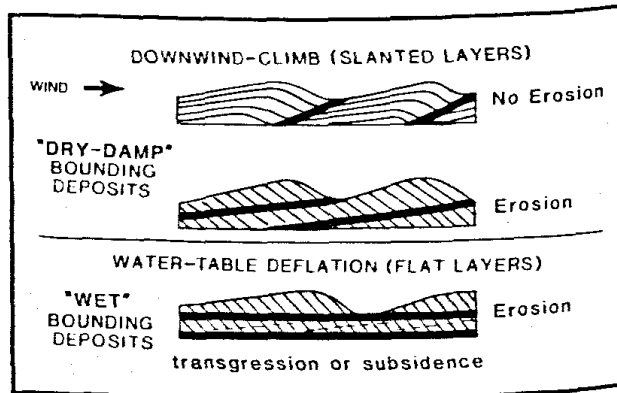


Fig. 14. Correlation hypotheses for net deposition and preservation of eolian deposits. Downwind-climb creates slanted layers for detailed correlation, whereas water-table deflation creates flat layers for larger-scale correlations. Internal composition of layers in the water-table deflation model are likely to be more complex than illustrated (e.g., consisting of downwind-climbing sequences).

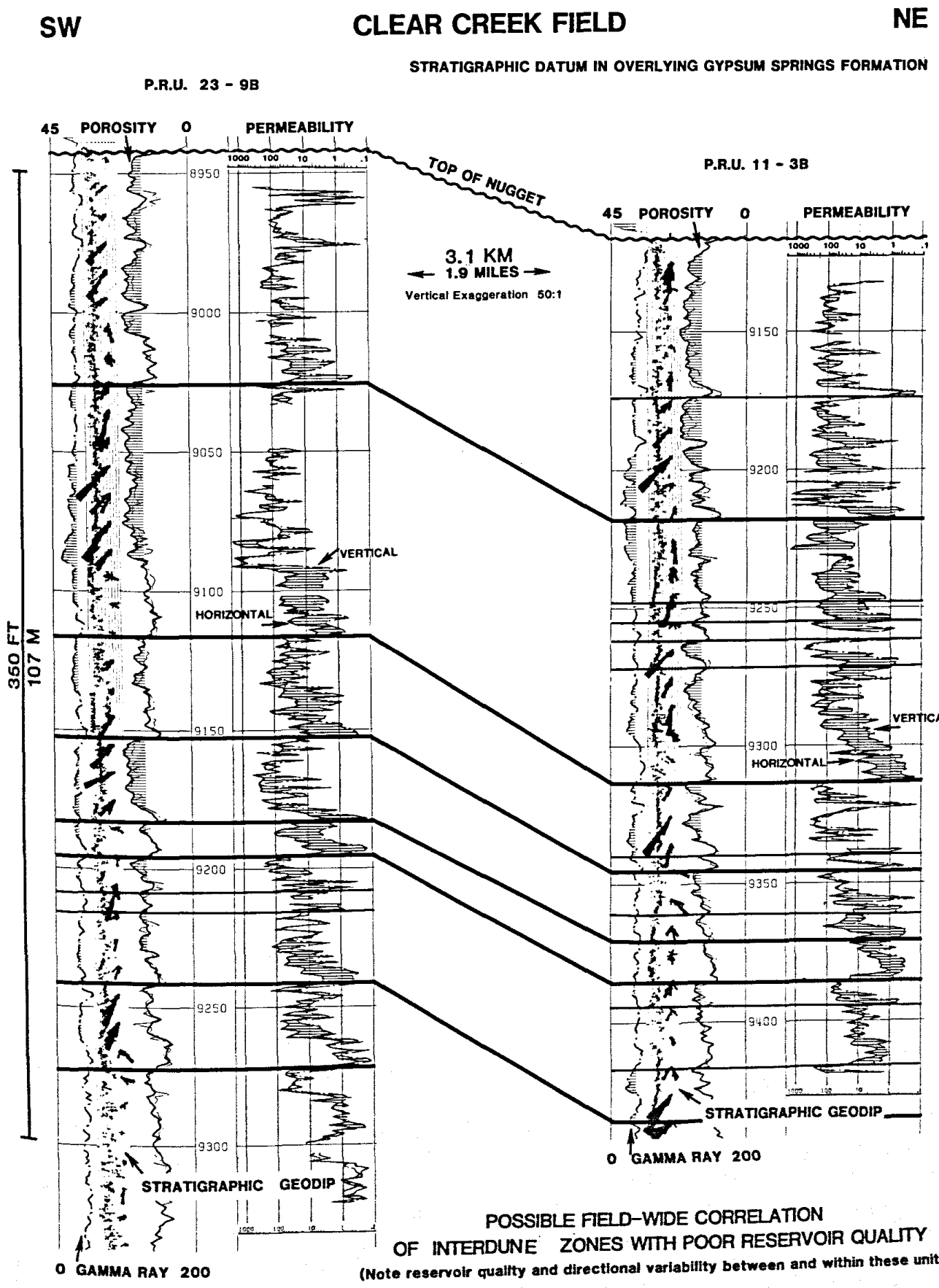


Fig. 15. Downwind-climb ("slanted-layer") correlation hypothesis applied at Clear Creek Field (from Lindquist, 1983).

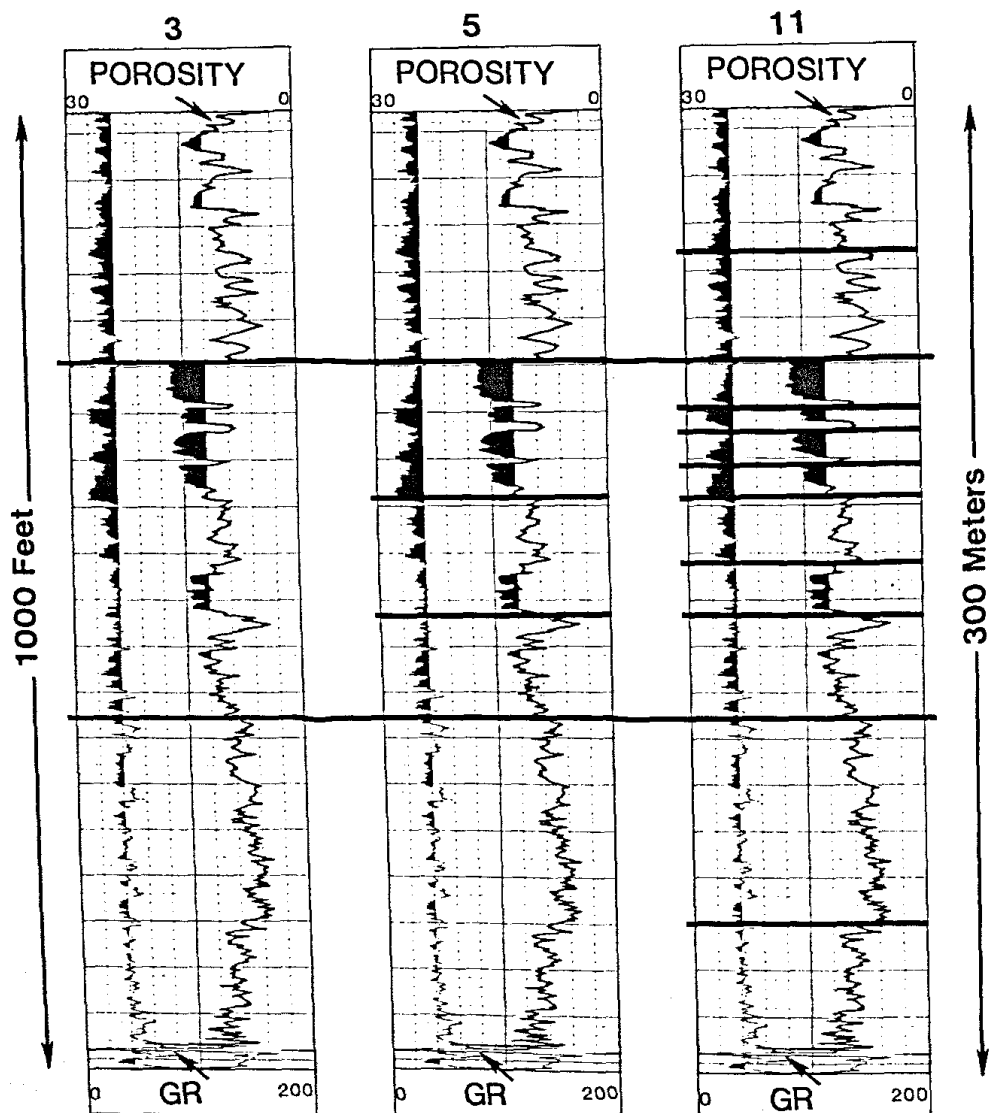


Fig. 16. "Flat-layer" models utilized in computer simulation studies of the Nugget Sandstone in Anschutz Ranch East Field. Porosity and gamma-ray curves are illustrated for 3, 5 and 11 layer representations of the W29-12 well.

layer") hypothesis of correlation was used to genetically subdivide the Nugget Sandstone at Anschutz Ranch East Field for computer simulations and reservoir modeling on several different scales. Three, five and eleven-layer subdivisions were made, based on genetic core description and reservoir quality characterization (Fig. 16). Numbers of layers utilized for simulations were restricted by computer time, space and expense limitations. An eleven-layer, "average well" (the W30-02 from Fig. 17) was utilized by Amoco's Production Department in simulation studies of a producing well responding to the injection of nitrogen for reservoir pressure maintenance from an injection well 80 acres or approximately 1050 ft (320 m) away (Clark, 1985). The nitrogen was being

injected to maintain reservoir pressure above the dew point to prevent in-situ hydrocarbon phase changes that would result in lesser recovery. Expected ideal response in the producing well would be to maintain or enhance hydrocarbon production. The W30-02 used as the model producer is, in reality, an injection well in the field. One layer of the W30-02 model (the high-porosity interval below the first correlation line in Fig. 17) had distinctly better reservoir properties than the other layers, and it was assumed for the model that reservoir properties were consistent over the entire lateral distance.

Clark's (1985) work showed that total production response to nitrogen injection would be dominated quickly (within a month or so) by that

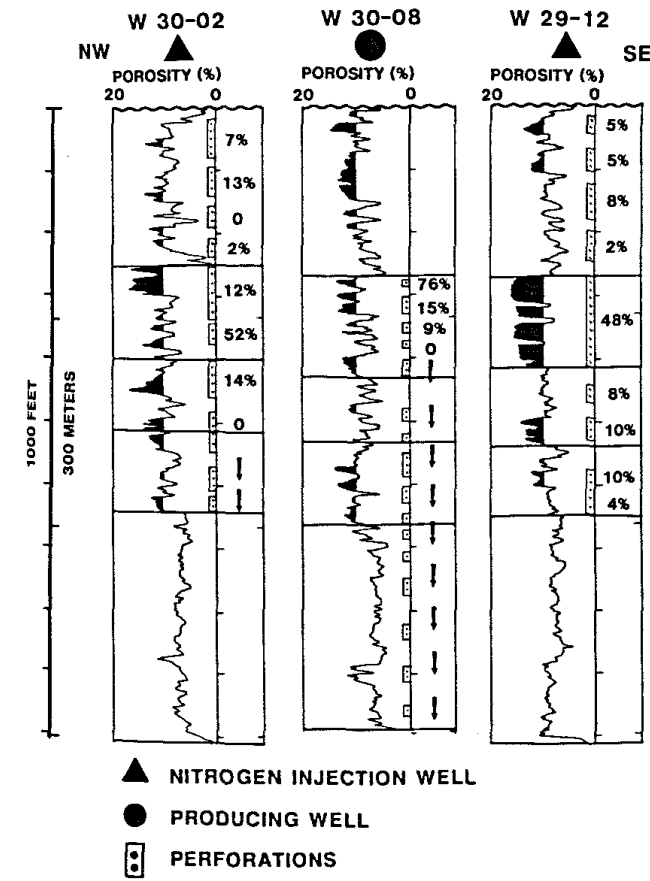


Fig. 17. Initial injection/production performance at Anschutz Ranch East Field in three wells parallel with depositional strike and maximum permeability trends. Log porosity >10% is shaded, and five "layers" are correlated (see Fig. 16). The proportionate amount of flow entering (injectors) or exiting (producer) the perforations is noted.

one layer in the producing well, but much of what would be produced would be recycled nitrogen from the injection well. The "pipeline" layer in the W30-02 model had 12.4% average core porosity compared with 6.9–10.9% for the other layers, and geometric average maximum horizontal permeability was 4.7 mD compared with 0.04–2.36 mD for the other layers.

Early Anschutz Ranch East production data from three wells oriented parallel with depositional strike (and parallel with maximum permeability trends) illustrate this rapid, layer-dominated performance that did occur (Fig. 17). The center producing well, W30-08, experienced nitrogen breakthrough early in its production history with 76% of the total production coming from one thin porosity interval within the same layer predicted by the model. Even parallel with depositional strike, lateral correlation of these small but obviously important porosity zones is problematic. "Layers" certainly are not homogeneous.

Lateral facies variability

Another factor that must be considered in modeling eolian reservoirs is lateral variability within layers or genetically correlative horizons. This complexity was discussed briefly with respect to

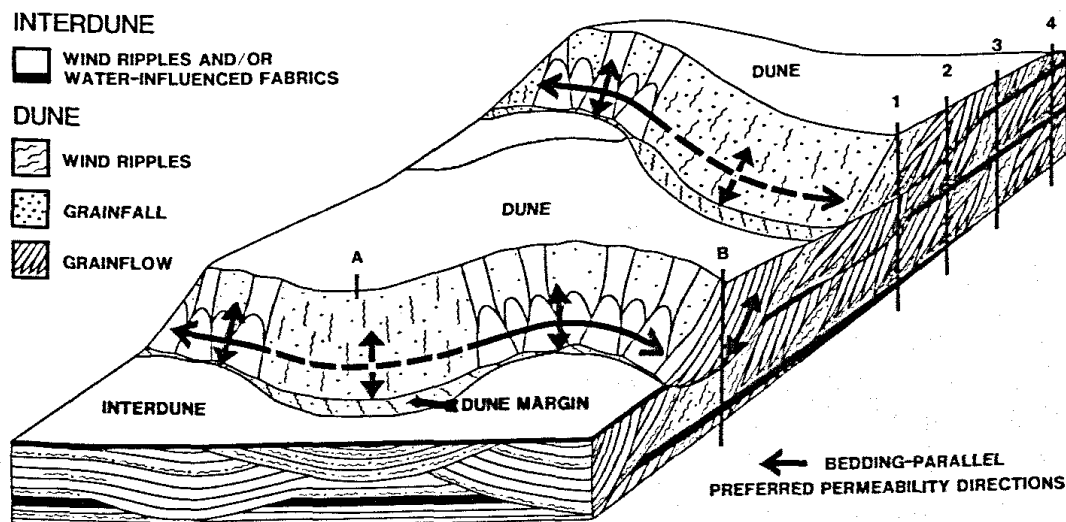


Fig. 18. Hypothetical, downwind-climbing, sinuous-crested eolian dune and interdune sequences. Note lateral and vertical variability in stratification type, preferred permeability components, and interdune barrier continuity. Cross-sections are in Fig. 19.

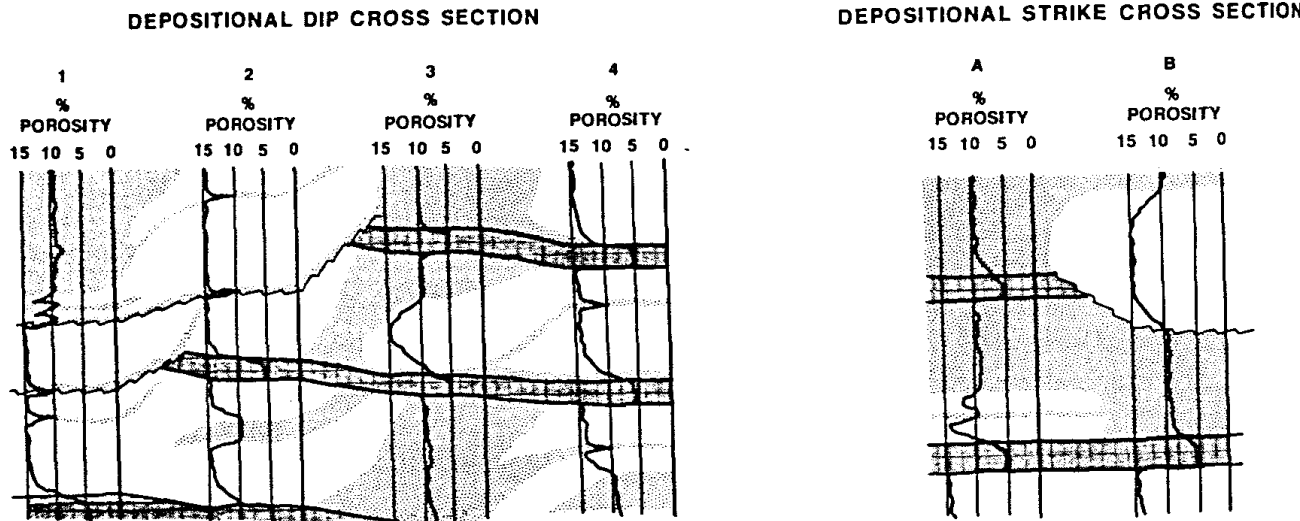


Fig. 19. Depositional-dip and depositional-strike hypothetical porosity cross-sections for Fig. 18. Grainflow deposits (plain) are arbitrarily assigned a porosity of 15%; rainfall and wind-ripple cross-strata (coarse stipple) 10%; and interdune deposits (fine stipple) 5%. Note lateral variability and compartmentalization in dune "layers" and potential communication between layers because of interdune erosional removal.

Figs. 15 and 17. Lateral variability in stratification types (both in depositional-dip and depositional-strike directions) for a hypothetical, sinuous-crested dune system is illustrated in Fig. 18, based in part on a published figure by Hunter (1977). Maximum permeability lines are superimposed, dashed where less continuous because of changes in stratification type. This is a downwind-climbing, "dry" interdune system, and each of the layers might be several tens of feet (± 10 m) thick. Two hypothetical "porosity log" cross sections are also presented (Fig. 19).

The depositional-dip section (Fig. 19) illustrates the theoretical downwind climb of interdune barriers, as well as the possible erosional removal of these barriers to create vertical communication from one layer to the next. If a wind-ripped interdune or dune-margin deposit is not developed at the erosional surface below the succeeding grainflow deposits, vertical interlayer communication might be locally excellent in those areas. Stratification types and reservoir properties are not likely to be consistent within layers, especially in a somewhat sinuous-crested system (the extensive preferred permeability direction in the dip cross-section is oriented perpendicular to the plane of the figure).

The depositional-strike section (Fig. 19) illustrates the theoretically flatter correlation of interdune deposits in this direction unless they are

removed by erosion. In this strike section, the extensive preferred permeability direction is parallel with the plane of the figure, but in some layers continuity is disrupted because of change in stratification type.

A subsurface example of lateral variability in layers is illustrated by two wireline porosity surveys

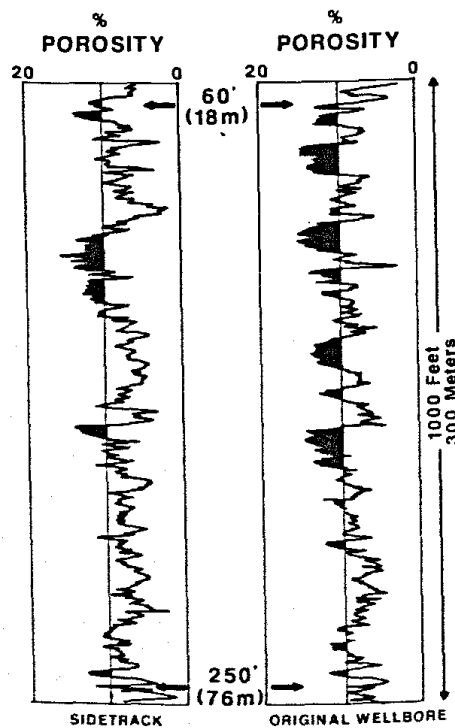


Fig. 20. Lateral porosity variability in twin wellbores at Anschutz Ranch East Field (W31-04A and W31-04B sidetrack).

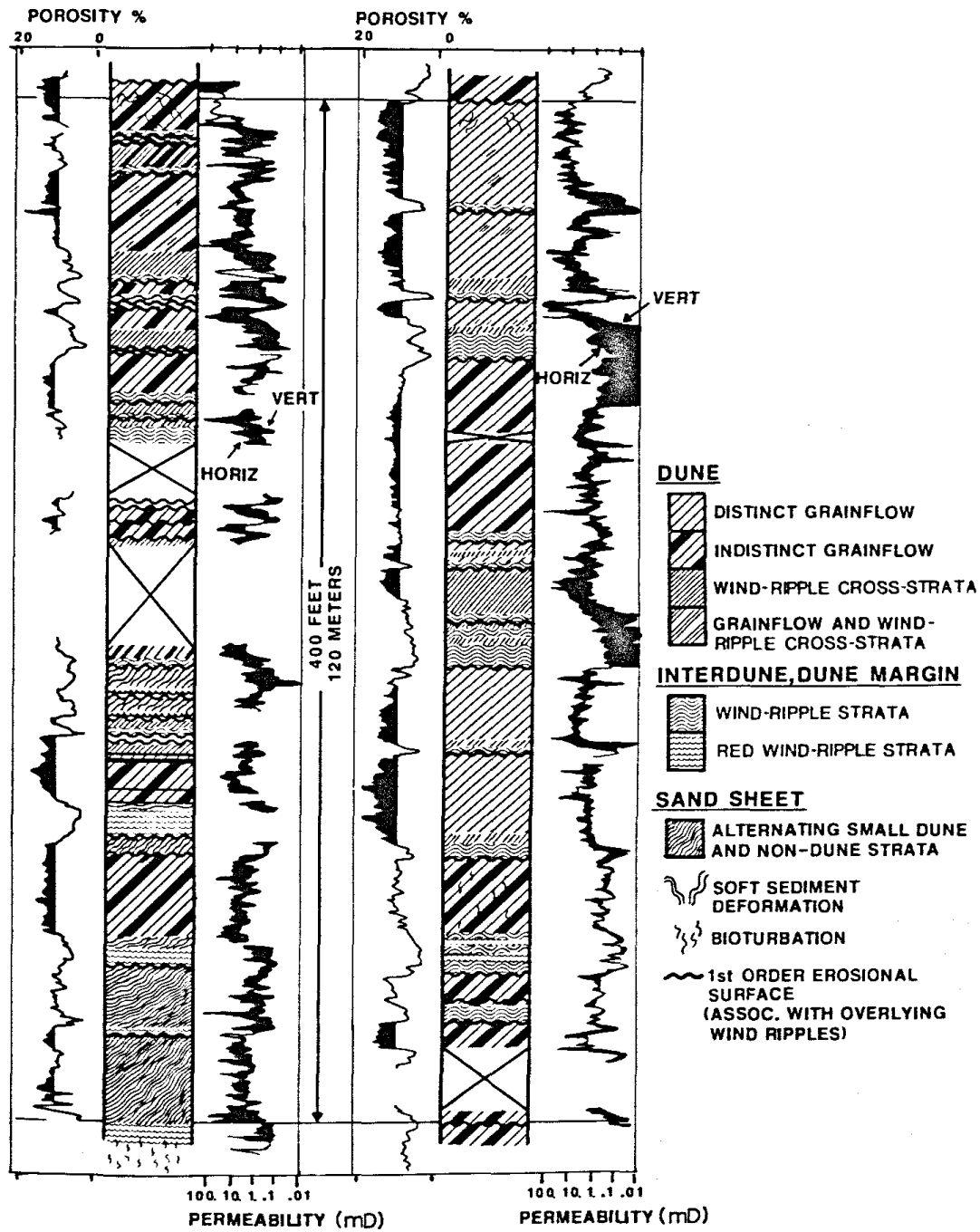


Fig. 21. Variability of stratigraphic sequence and reservoir properties within the middle Nugget interval of Anschutz Ranch East Field (W20-06 on left and W30-16 on right). Porosity > 10% is shaded, as is the difference between vertical and horizontal whole-core permeability. Descriptions have been somewhat simplified for the resolution of the figure.

from Anschutz Ranch East twin wellbores approximately 60 ft (18 m) apart at the top and 250 ft (76 m) apart at the bottom (Fig. 20). Note the differences in porosity and presumably permeability over distances comparable to urban homesites. The wells are oriented obliquely with respect to depositional strike.

Lateral variability within the middle 400 ft (122 m) at Anschutz Ranch East Field is exemplified by a comparison of core descriptions and core

analyses from two wells 1.5 mi (2.4 km) apart in a depositional dip direction (Fig. 21). The poorer well on the left contains only small dune sets with the indistinct type of grainflow cross-strata, whereas the better well on the right has larger dune sets with visually distinct grainflow cross-strata. Associated interdune deposits in the well at left also are commonly redder and finer grained, showing more evidence of the presence of water in the depositional environment.

Structural applications of stratigraphic concepts

Problems of structural interpretation can be solved in some areas by utilizing stratigraphic layering and correlation concepts. Structural models for Anschutz Ranch East Field were refined by utilizing a computer program to correct measured thickness wireline log data to true stratigraphic thickness, representing a perpendicular penetration of the formation (Fig. 22). The program works by mathematically removing the effects of formation dip and borehole deviation that can result in oblique formation penetrations and a stratigraphically "stretched" representation on log data. Correction factors were then applied to computer-plotted depth scales for each curve to generate synthetic true stratigraphic thickness logs.

Figure 23 contains a porosity and gamma-ray log plot from a well that penetrates an overturned fold filled with hydrocarbons. It is important to know what stratigraphic parts of the formation are intersected along the wellbore to determine the exact location and geometry of the steeply dipping and overturned structural limb in the subsurface. That, in turn, defines the exact location of hydrocarbon reserves with respect to surface leases.

The upper part of the sequence in the example is normally penetrated, a portion near the overturn is penetrated parallel with bedding, and the lower part is inverted. The inverted section below the point of overturn symmetry has been stratigraphically restored and correlated back to the normal section, based on the vertical porosity zonation for the field. Both the original measured-depth log and the stratigraphically "cor-

rected" survey are shown at the same vertical scale. Corrections have been substantial, especially near the overturn and in the inverted section. It can be concluded that a "mirror-image" penetration of the upper 450 ft (138 m) of Nugget stratigraphy has occurred along this wellbore. Therefore at the point of overturn, the top of the formation is approximately 450 ft (138 m) laterally from the leading edge of the fold.

The technique can be used iteratively until a reasonable stratigraphic representation is attained, enabling the user to determine structural dip magnitudes and azimuths for steeply dipping and overturned limbs where structural dipmeter data are poor. Care must be taken to account for possible major faulting that can result in repeated or missing section, and the technique is easiest to use where no major deformational thinning is suspected. The procedure does not provide a *unique* solution, but rather confirms a *reasonable* solution, if all other data fit the dip scenario chosen.

Illustrated in Fig. 24 is an example where true stratigraphic thickness restoration provided information regarding fault displacement. The corrected section illustrates the correlation of prominent porosity zones in two wells, one of which is stratigraphically "stretched" and contains a major faulted interval. Utilizing a first-pass, simple straight-limb deformational model, the well was stratigraphically corrected assuming a constant 35° dip for the upper two-thirds of the formation above the fault zone and a constant 65° dip for the bottom one-third below the fault zone. The fault location in the wellbore corresponds to a zone of block overlap where major movement and realignment of deformed material must occur in this model. A reverse sense of fault movement is required to attain the dip scenario configuration with respect to the fixed wellbore location, and the amount of offset can be quantified.

Conclusions

Even though eolian formations are heterogeneous and complex reservoirs, the combined use of core, conventional log, and dipmeter data with a coherent depositional, diagenetic and tectonic

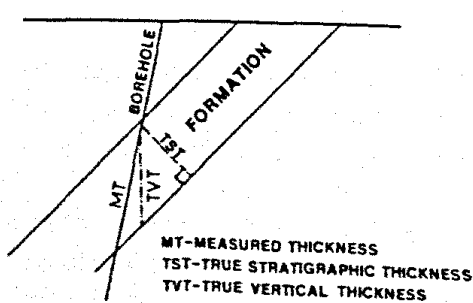


Fig. 22. Relationship of true stratigraphic thickness (TST), true vertical thickness (TVT) and measured thickness (MT) in deviated boreholes penetrating dipping strata.

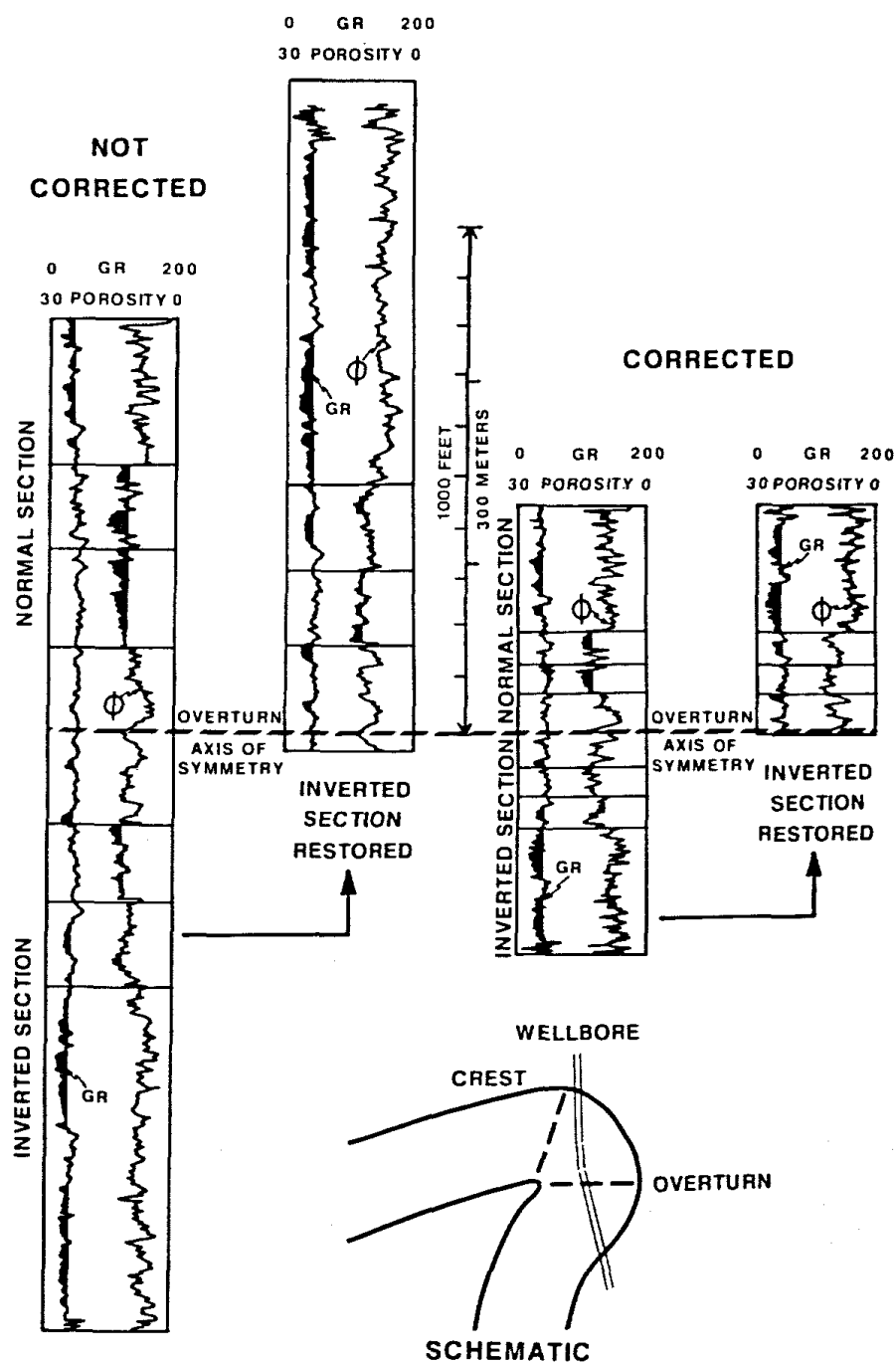


Fig. 23. True stratigraphic thickness restoration of porosity and gamma-ray log data from a well penetrating an overturned fold. Both the stratigraphically corrected (true stratigraphic thickness) and uncorrected (measured thickness) representations are at the same vertical scale.

model enables us to develop such reservoirs in a more efficient manner, even in structurally complex terrains.

The productive Jurassic Nugget Sandstone of the Utah-Wyoming thrust belt can be modeled on different scales as a predominantly cross-stratified, layered sandstone system with lateral variability within layers. Most extensive (bedding-parallel) preferred permeability trends are ori-

ented primarily NW-SE, perpendicular to the predominant southwesterly depositional cross-strata dip direction, but tectonic events have reoriented permeability components to varying degrees.

Locally and on a small scale, the downwind-climb (slanted-layer) hypothesis is an appropriate model to use for correlation. On a larger scale, the water-table deflation (flat-layer) hypothesis works well for correlation and modeling where laterally

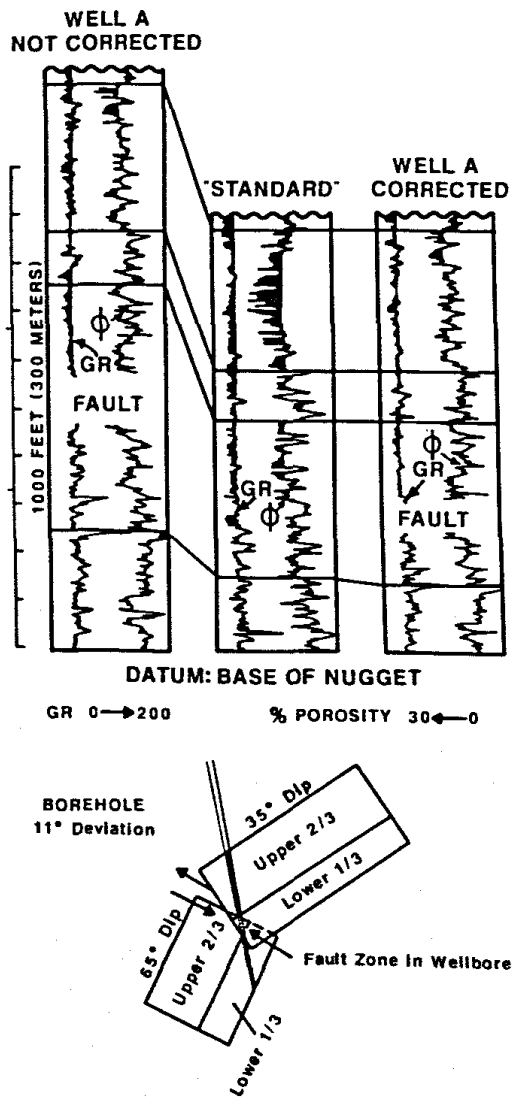


Fig. 24. True stratigraphic thickness restoration of porosity and gamma-ray log data from a well on a reverse-faulted fold flank. The corrected and uncorrected versions are compared to a "standard" Nugget penetration from the immediate vicinity.

consistent changes in depositional sequence have occurred through time. Combinations of core, dipmeter, porosity log, and gamma-ray data are suitable for making correlations.

Reservoir quality variability within and between layers is caused primarily by the range of stratification types associated with different dune morphologies and eolian subenvironments. Over the depth range of 7500–15,000 ft (2286–4572 m), Nugget dune grainflow cross-strata can have porosity as high as 25% and horizontal permeability greater than or equal to a Darcy. Connate fluids in these large pore systems can be easily displaced to low (< 10%) irreducible values. In

contrast, associated wind-ripple deposits (as dune cross-strata or as lower-angle interdune beds) can have porosity as low as 3% and horizontal permeability less than 1 mD. Pore systems are smaller, and fluids are less easily displaced in wind ripple strata.

Nugget wet interdune and non-dune facies are potential vertical barriers in the system, with porosity as low as 2% and permeability of just hundredths of milliDarcies. These facies probably retain at least 60–70% irreducible connate water saturation, and the movable portion is not easily displaced through the small pore throats.

Post-depositional, facies-related diagenetic and tectonic modifications to Nugget reservoirs include cementation by quartz, ferroan and non-ferroan carbonates, chlorite and illite; dissolution of silicates and carbonates; compaction and pressure solution; alteration of hydrocarbons; and formation of gouge-filled micro-faults and intermittently open fractures. Effects of these events on reservoir quality are, at most, just locally significant compared to the importance of depositional textural parameters on porosity and permeability.

Nugget stratigraphic models have been used successfully in reservoir simulation studies to predict and match production performance. In structural modeling studies, they have also been used to determine possible structural configuration in areas of complex deformation and to quantify fault displacements.

Acknowledgments

The author wishes to thank Amoco Production Company for permission to publish this paper, as well as the Journal of Petroleum Technology for permission to reproduce several figures previously published in 1982 and 1983. Data incorporated here were generated primarily from 1981 through 1983, except for more recent simulation model results by Terry Clark. Jeff Lelek worked on initial structure models at Anschutz Ranch East Field where true stratigraphic thickness restoration applications have been so successfully used. Harvey Meyer and Joe Applegate coordinated computer requirements for running the programs. Dennis Prezbindowski of International Petrology Re-

search provided hydrocarbon fluorescence observations on selected samples, and Al Marlowe of Amoco Denver performed NMR analyses. Many other individuals in Amoco's Denver office and Tulsa Research Lab shared their time and expertise on related topics.

Mark W. Longman and Charles E. Bartberger reviewed early drafts of this paper and offered helpful comments. I am most grateful, as well, to Earle F. McBride, Gary Kocurek, Chris Peterson, and Jim Frank who reviewed the later versions. Mike Ambrosio, Marilyn Cowhick and Jerry Daly assisted with much of the drafting, and Lydia Morris typed the manuscript.

References

- Ahlbrandt, T.S. and Fryberger, S.G., 1981. Sedimentary features and significance of interdune deposits. In: F.G. Ethridge and R.M. Flores (Editors), Recent and Ancient Nonmarine Depositional Environments. Soc. Econ. Paleontol. Mineral., Spec. Publ., 31: 293-314.
- Blakey, R.C., 1988. Basin tectonics and erg response. In: G. Kocurek (Editor), Late Paleozoic and Mesozoic Eolian Deposits of the Western Interior of the United States. *Sediment. Geol.*, 56: 127-151 (this volume).
- Clark, T.J., 1985. The application of a 2-D compositional, radial model to predict single well performance in a rich gas condensate reservoir. Society of Petroleum Engineers preprint SPE 14413, Las Vegas.
- Fryberger, S.G., Ahlbrandt, T.S. and Andrews, S., 1979. Origin, sedimentary features, and significance of low-angle eolian "sand sheet" deposits, Great Sand Dunes National Monument and vicinity, Colorado. *J. Sediment. Petrol.*, 49: 733-746.
- Fryberger, S.G., Al-Sari, A.M. and Clisham, T.J., 1983. Eolian dune, interdune, sand sheet, and siliciclastic sabkha sediments of an offshore prograding sand sea, Dhahran area, Saudi Arabia. *Bull. Am. Assoc. Pet. Geol.*, 67: 280-312.
- Helmold, K.P. and Loucks, R.G., 1985. Origin of high-permeability reservoirs in upper Minnelusa sandstone (Permian), Powder River basin, Wyoming and Montana. *Bull. Am. Assoc. Pet. Geol.*, 69: p. 264 (abstract).
- Hunter, R.E., 1977. Basic types of stratification in small eolian dunes. *Sedimentology*, 24: 361-387.
- Hunter, R.E., 1981. Stratification styles in eolian sandstones: some Pennsylvanian to Jurassic examples from the western interior U.S.A., In: F.G. Ethridge and R.M. Flores (Editors), Recent and Ancient Nonmarine Depositional Environments. Soc. Econ. Paleontol. Mineral., Spec. Publ., 31: 315-329.
- Kocurek, G., 1981. Significance of interdune deposits and bounding surfaces in aeolian sand dunes. *Sedimentology*, 28: 753-780.
- Kocurek, G. and Dott Jr., R.H., 1983. Jurassic paleogeography and paleoclimate of the central and southern Rocky Mountains region. In: M.W. Reynolds and E.D. Dolly (Editors), Mesozoic Paleogeography of West-Central United States, Rocky Mountain Paleogeography Symposium 2. Rocky Mountain Sect., Soc. Econ. Paleontol. Mineral., pp. 101-116.
- Kocurek, G. and Nielson, J., 1986. Conditions favorable for the formation of warm-climate eolian sand sheets. *Sedimentology*, 33: 795-816.
- Krystnik, L.F., Andrews, S. and Fryberger, S.G., 1985. Impact of early diagenesis of eolian reservoirs, Great Sand Dunes National Monument, Colorado. *Bull. Am. Assoc. Pet. Geol.*, 69: p. 276 (abstract).
- Lindquist, S.J., 1983. Nugget formation reservoir characteristics affecting production in the overthrust belt of southwestern Wyoming. *J. Pet. Technol.*, 35: 1355-1365.
- Loope, D.B., 1985. Episodic deposition and preservation of eolian sands: a late Paleozoic example from southeastern Utah. *Geology*, 13: 73-76.
- Marzolf, J.E., 1988. Controls on Late Paleozoic and early Mesozoic eolian deposition of the western United States. In: G. Kocurek (Editor), Late Paleozoic and Mesozoic Eolian Deposits of the Western Interior of the United States. *Sediment. Geol.*, 56: 167-191 (this volume).
- Peterson, J.A., 1980. Permian paleogeography and sedimentary provinces, west central United States. In: T.D. Fouch and E.R. Magathan (Editors), Paleozoic Paleogeography of West-Central United States, Rocky Mountain Paleogeography Symposium 1. Rocky Mountain Sect., Soc. Econ. Paleontol. Mineral., pp. 271-292.
- Rubin, D.M. and Hunter, R.E., 1982. Bedform climbing in theory and nature. *Sedimentology*, 29: 121-138.
- Stokes, S.L., 1968. Multiple parallel-truncation bedding planes —feature of wind-deposited sandstone formations. *J. Sediment. Petrol.*, 38: 510-515.
- Walker, T.R., 1979. Red color in dune sand. In: E.D. McKee (Editor), A Study of Global Sand Seas. U.S. Geol. Surv., Prof. Pap., 1052: 61-81.
- Warner, M.A., 1980. Source and time of generation of hydrocarbons in Fossil Basin, western Wyoming thrust belt. *Bull. Am. Assoc. Pet. Geol.*, 64: p. 800 (abstract).